AMERICAN UNIVERSITY OF BEIRUT

MODELING THE PHONON HEAT TRANSPORT IN SEMICONDUCTOR SUPERLATTICES

by

ZEINAB HASSAN HARAJLI

A thesis
submitted in partial fulfillment of the requirements
for the degree of Master of Science
to the Department of Physics
of the Faculty of Arts and Sciences
at the American University of Beirut

Beirut, Lebanon
September 2016

AMERICAN UNIVERSITY OF BEIRUT

MODELING THE PHONON HEAT TRANSPORT IN SEMICONDUCTOR SUPERLATTICES

by

ZEINAB HASSAN HARAJLI

Approved by:

Dr. Michel Kazan, Assistant Professor — Advisor
Physics

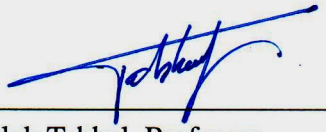

Dr. Malek Tabbal, Professor — Committee Member
Physics

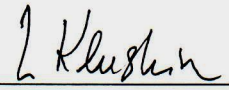

Dr. Leonid Klushin, Professor — Committee Member
Physics

Date of thesis defense: September 26, 2016

AMERICAN UNIVERSITY OF BEIRUT

THESIS, DISSERTATION, PROJECT RELEASE FORM

Student Name: HARAJLI (Last) Zeinab (First) Hassan (Middle)

☒ Master's Thesis ○ Master's Project ○ Doctoral Dissertation

☒ I authorize the American University of Beirut to: (a) reproduce hard or electronic copies of my thesis, dissertation, or project; (b) include such copies in the archives and digital repositories of the University; and (c) make freely available such copies to third parties for research or educational purposes.

☐ I authorize the American University of Beirut, to: (a) reproduce hard or electronic copies of it; (b) include such copies in the archives and digital repositories of the University; and (c) make freely available such copies to third parties for research or educational purposes after :

One ---- year from the date of submission of my thesis, dissertation, or project.
Two ---- years from the date of submission of my thesis, dissertation, or project.
Three ---- years from the date of submission of my thesis, dissertation, or project.

Zeinab Harajli — Sep 26, 2016

Signature Date

This form is signed when submitting the thesis, dissertation, or project to the University Libraries

ACKNOWLEDGEMENTS

After an intensive period of work, today is the day: writing this note of thanks is the finishing touch on my thesis. It has been a period of intense learning for me, not only in the scientific arena, but also on a personal level. So now, only one day before reaching the end of my masters' years, I would like to reflect on the ones who have supported and helped me so much throughout this period.

"Trust in the Lord with all your heart, and lean not on your own understanding, in all your ways acknowledge Him, and He shall direct your paths."

First and foremost, I would like to thank my loving Creator for all his generous giving though I never deserved any.. Thank you Allah.. for hearing my prayers, giving me when I was most in need, and guiding me to people blessed by traces of your kindness. I hope to always be fortunate enough to have faith and belief in my heart, and have the delight of visiting holy Mekkah, the beautiful shrines of our sacrificing imams, from whom I learn true humanity and noble faith to truth, and maybe someday also visit the holy lands of Palestine.

I would like to thank my amazing advisor... Whose impact on me I shall never forget. Professor Michel Kazan, you supported me greatly and were always willing to help me. Your patience, infinite thoughtfulness and understanding simply leave me speechless. you were so nice, professional and dedicated to scientific research and learning. I am proud I had the chance to learn with such an inspiring person who makes even the most difficult tasks of research interesting and the simplest of concepts challenging! I hope to always have the chance to work with you in the future, and always learn from your excellent scientific skills.

I would like to thank my instructors, professor Jihad Touma, and professor Leonid Klushin. Their simply inspiring way of teaching the most complicated courses makes every session an exciting challenge. You definitely provided me with the tools of creativity and critical thinking that I needed to choose the right direction and successfully complete my thesis. The effect I had from my experience with you will always be curved in my mind. I also thank professor Malek Tabbal for his assistance as a committee member, and the amazing scientific meetings and discussions he assembled last summer for our group of material science researchers.

To my mother, who has a special way of loving us, by helping me everyday in everything I do, without her sacrifices for my future I would have never reached success. To my dearest father, whose love I always touch in his endless giving, thoughtfulness and everything he does for us, every day. My sisters Zahraa and Roukaya, my brother Ahmad, I hope someday I can also watch you do accomplishments in life and make me proud.

To my dear husband, Mohamad, whose understanding and continuous encouragement helped me pass every night of studying and every day of exams alive. Hoping to come see your thesis defense soon!

My sweet daughter Fatima, without you this thesis would have been completed two years ago.. Yet you are the most precious blessing I have and you will be worth the sacrifice..

Someday you will be a smarter girl than your mother, you can then take this thesis down from some upper shelf, dust it, and tell me what you think of it.
I would also like to thank my friends, Fatima Mahdi, Fatima Hashem, Ali Asghar and particularly single out my 'peer advisor' Ali Abou khalil, I want to thank you for your excellent advice and for all of the opportunities I was given to conduct my research and further studies thanks to your personal guidance and wise opinion. Your instructions before every step I did in my master's study made my life at AUB perfectly smooth and my university concerns always resolved. My wishes for you to have the best of luck and receive God's guidance and blessings in your decisions just like I received yours and more.
Finally, I dedicate my work to my only love, my beautiful country Lebanon. I dream every day of seeing peace and unity among all its parties. We are all descendants of this heaven of mighty Cedars and pure Olive trees, and this treasure is enough to make us neglect all other differences and conflicts between us. My lifetime dream is to see Beirut, and all other cities, valleys and mountains of our region, governed only by people who are faithful to attaining our hopes for peace and continuous development.
Zeinab Harajli Sep26, 2016

AN ABSTRACT OF THE THESIS OF

Zeinab Hassan Harajli for Master of Science
Major: Physics

Title: MODELING THE PHONON HEAT TRANSPORT IN SEMICONDUCTOR SUPERLATTICES

Understanding the laws that govern the phonon heat transport at atomic interfaces in crystalline superlattices has long been viewed as a key step toward efficient thermal-management strategy for high-performance superlattice-based thermoelectric, microelectronic, and optoelectronic devices. Therefore, several experimental studies on the phonon thermal conductivity in superlattice structures have been carried out, and many numerical techniques describing the phonon heat transport in multi-layer systems have been developed. Experimental studies have demonstrated that, in some circumstances, the phonons in a superlattice can propagate ballistically without being scattered at the interfaces as if the superlattice is a bulk material with no interfaces. This phonon mechanism is known as the coherent phonon transport mode, while the phonon heat transport mode in which phonons experience scattering at the interfaces is known as the incoherent phonon transport mode. Experiments have also demonstrated that when the interfaces between the layers that form the superlattice contain low amounts of irregularities, the superlattice cross-plane thermal conductivity presents a minimum value for a particular period thickness. However, in the case of diffusive interfaces, the cross-plane thermal conductivity increases monotonically with increasing the period thickness. Most theories for the superlattice thermal conductivity either rely on the solution of the Boltzmann transport equation that treats the phonons as particles or are based on the assumption that the phonons are plane waves. The existing Boltzmann models involve a rate at which particle-like phonons are scattered by interfaces. Thus, according to all Boltzmann models, the superlattice cross-plane thermal conductivity decreases monotonously as the interface density increases, which disagrees with the experimental measurements that demonstrated a minimum in the curve describing the cross-plane thermal conductivity versus the period thickness. On the other hand, by invoking the interference of phonon plane waves within thin periods, the models that consider the phonons as plane waves could describe the experimentally observed cross-plane thermal conductivity trend only at a period thickness smaller than a few tens of Angstroms. At relatively large period thickness, these models overestimate the superlattice thermal conductivity. Thus, so far, the physics of the phonon heat transport in superlattices could not be fully explained by a single model. Indeed, it is highly desirable to have a wide scope model that can accurately predict the dependences of the

period thickness and interface conditions on the thermal conductivity and phonon heat transport mode in superlattices. With such a theoretical tool in hand, one can gain insight into the physics of phonon heat transport across atomic interfaces and rationally design superlattices for many technological applications. In this thesis, we intend to develop an original approach for the determination of the phonon cross-plane thermal conductivity and heat transport mode in superlattices. It will be based on the interpolation between two Boltzmann models: an incoherent Boltzmann transport model assuming that the cross-plane thermal conductivity of the superlattice is a weighted average of the thermal conductivities of the two bulk materials that form the superlattice period with the additional contribution of the interface thermal resistance, and a coherent Boltzmann transport model based on the assumption that the superlattice is a bulk material, free of interfaces, characterized by phonon dispersion relations determined by the Brillouin zone folding effects of the superlattice. We will assess the reliability of the developed approach with reference to reported experimental data.

CONTENTS

CHAPTER I

INTRODUCTION

Understanding the thermal conductivity and heat transfer processes in thin films and superlattice structures of semiconductors is critical for the development of microelectronic and optoelectronic devices as they constitute a crucial basis in these devices [1] as well as in low-dimensional thermoelectric and thermionic devices [2]. The establishment of measurements for the thermal conductivity of superlattices experimentally requires understanding heat conduction in these systems. A theory describing superlattice heat transfer presents a key step in improving the performance of devices. Although obtaining a complete theory of lattice thermal conductivity is possible in principle, complicated crystal vibration spectra and anharmonic forces in lattices and the approximations in solving the Boltzmann equation are formidable barriers to progress. Studies demonstrate that the thermal conductivity of a superlattice could be much lower than that estimated from the bulk values of its constituent materials, and even smaller than the thermal conductivity values of the equivalent composition alloys. To establish a theoretical model that explains thermal behavior in these structurea, models for the thermal conductivity of superlattices, based on the Boltzmann transport equation [2], and phonon group velocity reduction [3], have been developed.

A. Heat Transfer and the Change of Materials' Properties in Nanoscale

Nanotechnology has become a major driver of information processing through storing data and transmitting it using microelectronics and nanowires. But electronic processors often generate heat that has to be controlled to maintain the standard temperatures of devices above which their function becomes inefficient and they get threatened by cor-

ruption. As devices get smaller, heat generation becomes compacted to smaller volumes, hence increasing density of heat generation and requiring better cooling processes[4]. For example, an intel Pentium4 chip dissipated 60 watts of energy over an area of 1cm2. To cool this chip and keep it at its maximum standard temperature of 120^oC, a fan much larger than the chip itself had to be used, which was a very unpractical cooling method that made an obstacle in the overall device size. In nanoscales, understanding heat transport always comes handy in improving efficiency of energy conversion, cooling and power generation [5]. Studies of thermoelectric devices controlled by nanostructures showed promising results in improving electrons energy and reduced heat loss [6]. Understanding the theory of heat transfer in nanoscale has become crucial in order to minimize heat formation and speed up heat conduction away from these devices [4]. It was for instance observed that superlattices, which possessed periodic properties, have formed a super-period, which was smaller than the original period in bulk sizes, and thus altered the phonon dispersion relation and thermal conductivity values. The study of heat transport has shown high dependence on the material's size, shape, orientation, imperfection and atomic content and placement. Heat transfer is basically due to coupled atomic vibration in crystals, which start by a temperature gradient leading to their excitation. the quantisation of these excitations leads to the concept of phonons. Phonons exist in two types: acoustic and optical. Acoustic phonons have low frequencies but high group velocities, while optical phonons have high frequencies, and generally they can't contribute directly to heat transfer. Moreover, heat transport by phonons at interfaces has shown two modes depending on the phonons' characteristics: Those with mean free path comparable to the inter-atomic spaces demonstrated an incoherent propagation and experienced scattering through their transfer, and those with a mean free path much larger than the lattice size propagated ballistically and coherently like waves. These modes will be interpolated together to form the general description of heat transfer through the lattice and to show how much each of these contributes to heat transfer in this thesis.

B. Generalities on the Terms Under Study

Before starting with the formalism of the problem this study addresses, it would be best to present some basic definitions of the fundamental concepts addressed in this thesis, just to keep best track of understanding the mathematics as things get complicated. These fundamentals include the meaning of heat transfer, nanoscale properties, superlattices and semiconductors.

- Heat Transfer The classical definition of heat energy transfer, as presented by Gang Chen, is described as "The energy flow through a material due to a change in temperature." [7]

- Nanotechnology National Nanotechnology Initiative defined nanotechnology as manipulation of materials of size between 1 to 100 nm. The sizes are much smaller than biological cells. Due to their promising properties, governments provided high funding on this domain of research.

- superlattices An important fabrication in nanoscale semiconductor systems is the superlattice, which is an artificial fabrication of periodic layers of thin films of a few nanometers thickness each. Superlattices presented excellent improvements in the properties of their constituent materials; they provided 100 times stronger shearing resistance, increased mechanical hardness, and higher thermal resistivity [8]. A basic property of superlattices was that they demonstrated a dramatic drop in thermal conductivity compared to similar bulk structures of same constituent materials.

- Semiconductors When superlattice layers are made of semiconductors, many new observations arise due to mismatch at interfaces and quantum size effects. Semiconductors form most of the materials used in superlattice fabrication, and represent a favourite candidate because of their flexibility in acoustic and optical properties. Accordingly, they will be the material under study in this thesis, and results will

basically be illustrated through the example of Silicon and Germanium alloy samples. In fact, almost all microelectronics are formed of silicon,[9] mainly because of its unique properties of mechanical stability, electrical isolation, and good thermal conduction.

- Phonons "A phonon is the quantum of crystal vibrational energy" [10] the concept of phonons is similar to the concept of photons which are the energy quanta of electromagnetic waves. In a very similar approach, mechanical waves are also quantized to phonons arising from the relative vibration of atoms. They conduct sound, which results from vibrations of up to $1011Hz$, as well as heat, which corresponds to vibrations above $1011Hz$ [11]. Understanding phonons is the basic key to thermal management and controlling heat transport.

C. Desire for a Complete Theory of Heat Transfer at Nanoscales

The recent advance in nanotechnology has brought new demands on the control of heat transfer at nanoscales. As devices get so minimal, reaching nanoscales, their dimensions become comparable to the wavelength of energy carriers inside them. This effect of size will have consequences on most of the laws governing energy transfer in these devices. The main interest in this thesis is the drastic drop in heat conduction leading to overheating when materials reach low dimensions which caused failure in first microchips due to increased heat dissipation density because of the minimized surface area in these fabrications. For example, a quantum cascade laser used in telecommunications and storing data was made of a superlattice of InAs/AlSb layers. Due to an unexpected drop in thermal conductivity, these lasers were limited in their performance due to heating problems [7]. Thus a theoretical study to provide an explanation of this experimental observation at low dimensions is required to maintain better control over fabrication of prod-

ucts, increase their durability and efficiency, and prevent heat damage. In principle, heat conduction takes place in a material when different energy carriers move between atoms. These energy carriers can be electrons, photons, or phonons [7]. This study focuses on heat transfer by phonons, which will be the dominant heat carriers in crystals of large band gaps where electrons cannot contribute to heat transfer. Many theories where developed for describing heat transport, and to describe the change in thermal conductivity at nanoscales. It was remarkably noticed that carriers demonstrated spatial dependence which showed that macroscopic heat transfer laws, which considered thermal conductivity to be just an intrinsic property of a material, became invalid at these sizes. Therefore, a need for new mechanisms to describe thermal properties aroused. Understanding the laws that control phonons carrying heat across lattices in low dimensions will indeed provide knowledge on the physics governing thermal conductivity of crystalline materials in nanoscale [12]. The study of phonon dynamics which will lead to the equations governing thermal resistivity starts with a Boltzmann distribution of the excited atoms inside a lattice, the variation in the number of excited modes due to a temperature gradient is then presented by Boltzmann's equation. Solving this equation will provide a formula for the number of excited modes, which, in addition to the frequency values obtained from the dispersion relation of a superlattice, gives the thermal conductivity as a function of temperature and other parameters depending on the properties of the material under study. A major factor that controls heat transfer is the phonon scattering. Scattering occurs inside a crystal due to many processes taking place in the lattice. Mainly, creation and annihilation of phonons is a major type of scattering resulting from the an-harmonic term in the potential existing between the crystal atoms. The presence of impurities also results in scattering of phonons at the location of these impurities, and finally, a major process that affects heat conduction at nano-scale is the phonon scattering by boundaries. The interaction between surface phonons and phonons inside the volume also causes a scattering to be accounted

for.

D. Thesis Problem

Out of the above aspects of heat transfer at nano-scale, a lot of theoretical demands as well as physical interest arise for explaining the new features in thermal conductivity in superlattices accurately. Hence, a new model for the derivation of thermal conductivity formula across superlattices will be presented. Explanation of the relaxation time of phonons scattered at interfaces in a superlattice in addition to other phonon processes will be demonstrated to determine the terms affecting their values. An approach to minimize thermal conduction across superlattices will be provided as a theoretical model that improves the efficiency of thermoelectric devices. Effects of interface properties and period values need to be studied too to provide insight on the physics governing phonon dynamics in nano-scale.

E. Literature Review

The study of thermal conductivity of materials has been an interesting topic for physicists in order to distinguish good conductors from good insulators, and to provide important tools for industry applications. As such, experimental and theoretical studies were carried out in order to describe heat conduction and the factors involved in its variation. The first theoretical studies of thermal conductivity focused on solving the Boltzmann equation for phonons transport. Two approaches were known; the variational method and the relaxation time approximation where each presented certain limitations. In the relaxation time approximation, phonon scattering was described through the relaxation time of each process. results were basically established by the work of Casimir in studying boundary scattering [13], Klemens gave an expression for isotope scattering and studied the dependence of

the Umklapp scattering on phonon vibrational spectrum, then Herrings studied normal processes relaxation times[14]. Debye and Peierls[15] predicted that thermal conductivity increases as a function of temperature until it reaches a maximum before it drops again. Carruthers[16] provided a thorough discussion of some of the processes and theories behind thermal conductivity of solids. Callaway was the first to give a complete theory describing thermal conductivity from solving a Boltzmann equation with relaxation time assumption. Although this model was based on rough approximations and contained many fitting parameters, it provided good fits with measurements at low temperatures. Further refinements were added through the work of Holland, Asen-Palmer et al. and Morelli et al. until the full theoretical description with no fitting parameters came to light. This improved model agreed to a large extent with experimental measurements of the lattice thermal conductivity for bulk materials and proved to be the most consistent model that can cover a large range of temperature. So far, the discussion summarizes the previous work concerning the lattice thermal conductivity of bulk semiconductor of simple crystal structure. With the advance in technology and industry, in addition to the need of miniaturization of devices and the emergence of semiconductors in various fields, bulk materials of more complex crystal structures along with new structures were fabricated such as thin-films, superlattices and nano-wires. The role of size and boundaries in reducing thermal conductivity were also treated thoroughly. Thermal properties of thin-films and superlattices have drawn increasing attention due to the demand of thermal management in the rapidly growing industries. Thermal management becomes more challenging as the power density and speed of integrated circuits keep increasing. As such, thermal conductivity of constituent thin-films becomes more important in the device design. Thin-films of high thermal conductivity are used in microelectronic and photonic devices in order to dissipate heat to avoid overheating of the device, whereas thermoelectric devices call for low thermal conductivity thin-films.Experimental measurements of thermal conductivity across

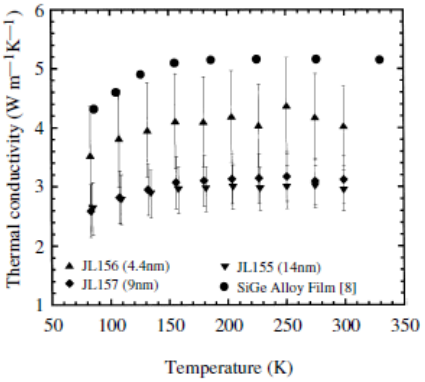

Figure 1: Temperature dependence of the thermal conductivity of undoped Si/Ge superlattices as well as SiGe alloy film[17]

superlattices have shown a drop of values of K(T) in materials which initially possessed higher values at bulk scales. Figure 1 presents an experimental measurement done on Si/Ge superlattices for the values of thermal conductivity as function of temperature, with a plot of thermal conductivity of the bulk silicon/Germanium alloy film. Experiments also showed that a decrease in heat conduction takes place as the period of a superlattice increases. Doping also appeared to lower thermal conductivity [15]. Measurements of thermal conductivity in superlattices started with Lee and co-workers [18] who measured the thermal conductivity of fully-strained Si/Ge superlattices. It was proven that all superlattices demonstrated lower thermal conductivity than their constituent bulks. Theoretically, three models were provided to describe phonon transport in semiconductor superlattices [10]. The first treats the phonons as totally incoherent particles and thus employs Boltzmann transport equation with appropriate boundary conditions [19]. This model gives good agreement with experimental data but fails for periods below 5 unit cells. The second model treats phonons as purely coherent waves [20]. Under this assumption, thermal conductivity in superlattices is calculated from the phonon dispersion curves. Predictions from this model for the very thin period limit agrees with the corresponding experimental data but deviations are strong for thick superlattices. The third group involves lattice dynamics which results in a temperature depen-

dent thermal conductivity similar to that of bulk materials as opposed to most of the experimental results. An analytical expression for the thermal conductivity of superlattices was derived by Alvarez and co-workers [21]. The authors proposed a simple expression that can predict in-plane and cross-plane values of the thermal conductivity of superlattices from an expansion of the Boltzmann equation with a combination of the acoustic mismatch and diffuse mismatch model for the thermal boundary resistance. Interpolation between the acoustic mismatch model and the diffuse mismatch model was done by including an adjustable specularity parameter p. A reasonable fit to the experimental values was provided by this model.

F. Roadmap

As a start, generalities on heat transfer in bulk semiconductors will be discussed, then an attempt to obtain an expression for thermal conductivity as a function of temperature is demonstrated starting with Boltzmann's transport equation of statistical behaviour of perturbed thermodynamic systems. An equation including thermal conductivity as a function of relaxation time of different phonon scattering processes will also be derived. The second step would be to obtain expressions for these relaxation times of each phonon scattering processes due to different interactions. Introducing temperature dependent heat capacity as well as temperature dependent Gruneisen parameter will be included in the study instead of the classical parameters. T-dependent parameters have shown great improvement on the accuracy of theoretical values of thermal conductivity. Finally, A computational code is used to plot the obtained values of this expression across a full temperature range (0-1000K) in order to match these values with experimental measurements. Then, a detailed study of heat transfer in superlattices will be demonstrated. An expression of thermal conductivity obtained from a modified Boltzmann equation that accounts for interfaces is first presented. then a detailed study of the approach

of finding a dispersion curve from the continuum theory of phonons in superlattices is done. Once the generalities on superlattices are demonstrated, heat transfer in these structures will be studied by two models. the first model suggests a coherent phonon transport in the superlattice while the second model presents an incoherent mode of phonon transport. Finally, a detailed interpolation is provided to account for both effects. After presenting the theoretical details, a representation of the obtained results will be discussed and matched with experimental measurements to prove the reliability of this model. In the last section a mesh of thermal conductivities of SiGe/SiGe superlattices of variable alloy compositions is presented to obtain the minimal thermal conductivity superlattice that can be ideal in thermoelectric applications.

CHAPTER II

GENERAL THEORY OF LATTICE THERMAL CONDUCTIVITY

Thermal conductivity is a fundamental transport parameter that is commonly used to characterize a broad range of materials and systems. A predictive theoretical approach to calculate the lattice thermal conductivity in these materials is of tremendous importance for modern science and technology. It would facilitate understanding of heat dissipation in microelectronics and nanoelectronics [22] as well as assist in material design for efficient thermoelectric refrigeration and power generation [23].

The study of the thermal properties of nano-materials requires understanding how energy propagates in this type of industrial system to optimize their properties. Many technological applications have emerged during the past two years to handle the heat at the atomic scale in numerous approaches of study. In semiconductors and insulators, heat is carried by the vibrating lattice. Above a few tens of Kelvin the behaviour of the lattice thermal conductivity of semiconductors is usually dominated by phonon-phonon scattering, which arises because of the anharmonicity of the interatomic potential. Considering phonons in semiconductors, three main approaches are provided to study phonon dynamics through crystal structures which lead to obtaining the dispersion relation controlling the energy of phonons. In order to find the dispersion relation, either a semi-classical approach can be considered, a quantum approach, or usage of molecular dynamics simulations. However, the quantum approach, known as the ab-initio treatment, requires extremely heavy calculation and Super computers for calculations [10]. And since the molecular

dynamics study doesn't provide physical insight nor describes theories, the study will proceed for the lattice dynamics by approaching phonons in the semi-classical treatment based on the elasticity theory. In this chapter, we start with generalities on crystal properties, then proceed to study crystal vibrations to derive the phonon energy and the Hamiltonian controlling their behaviour. Then we describe phonon propagation by the Boltzmann equation, which presents a model for the spatial and temporal variations of the distribution function of phonons. The variations are controlled by the relaxation times of different phonon scattering processes. These will be derived from the study of the processes phonons undergo during their propagation in the crystal. Finally, we can derive the thermal conductivity formula in terms of the solution obtained from solving the Boltzmann equation. In the following section we introduce phonons, their properties and transport mechanisms as an introduction to the details of calculating rates of heat transfer by these carriers.

A. Quantum Treatment of Phonons

Phonons are present in crystalline materials which have a periodicity in their structure. Materials that do not have a translational symmetry, such as amorphous solids or soft matter, will not present phonon properties and are rather studied by the classical conduction phenomena. In general, phonons are defined as the quanta of the vibrational energy of the crystal lattice. This was mathematically deduced by a similar study of photons, in which we take into account creation and annihilation operators of phonons. Phonons will present the normal modes of vibrations, and will be subject to classical mechanics' laws. They will propagate from the heat source to the heat sink as vibrational waves carrying thermal energy inside the crystal lattice. Phonons will contribute to heat flow over a wide frequency range by undergoing collisions due to different interactions altering the heat transfer. These collisions are known as phonon scattering processes. The average time between phonon scat-

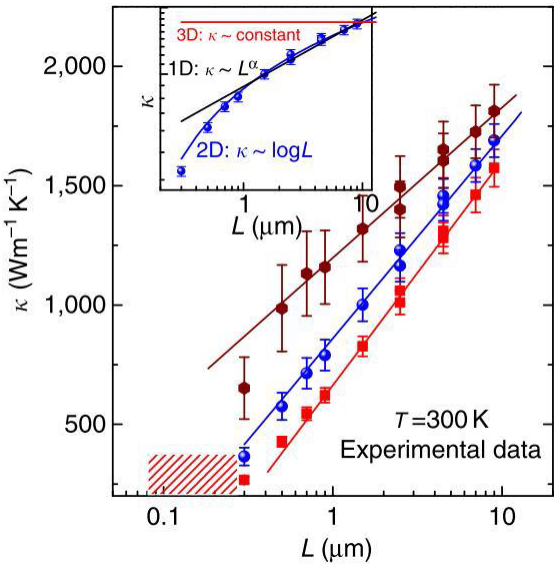

Figure 2: thermal conductivity as a function of size in Graphene monolayers[24]

terings will be defined as the relaxation time of the corresponding scattering processes, and will be critical for evaluating the thermal conduction in crystals. When a vibration has a close characteristic time to the relaxation time, Fourier's law is no longer valid to describe heat transfer, and Boltzmann's equation that describes the evolution of a system after applying a temperature gradient will be considered instead so as to account for the temporal evolution of phonons. The same problem arises when the size of the system becomes comparable to the mean free path of the phonons, which is defined as the average distance travelled by phonons before they scatter.

At low dimensions, phonons will become dependent on geometry, as illustrated in figure 2 which represents the thermal conductivity as a function of size in Graphene layers [24]. Indeed, the mean free path in bulk Graphene was much higher before the length became in nanoscale, which justifies the logarithmic dependence of the curve. Before we focus on the characteristics of phonons, it is important to start with a derivation of the quantization of lattice vibrations which lead to the presentation of phonons as the fundamental heat carriers.

The concept of phonons arises from the quantum mechanical model of lattice vibrations as a quantum mechanical harmonic oscillator. We present the quantum treatment of lattice vibrations in semiconductor crystals by starting with a linear chain of N atoms. The atoms are located at a distance $x_1, x_2, ..$ from equilibrium positions, and the potential energy of the lattice is essentially dependent on the position of the atoms of the lattice. Taking lattice vibrations to be a small increase in energy which can thus be found from a Taylor expansion of the potential energy around equilibrium in terms of atomic displacements

$$\phi = \phi_0 + \sum_{lk\alpha} \phi_\alpha(lk) u_\alpha(lk) + \frac{1}{2} \sum_{lk\alpha, l'k'\beta} \phi_{\alpha,\beta}(lk, l'k') u_\beta(l'k') + .. \tag{1}$$

where $u(lk)$ is the displacement of the k^{th} atom found in the l^{th} unit cell. α is the direction in Cartesian coordinates. The first term of the expansion is the equilibrium value of the energy. The second term is taken to be zero in order to get a minimum in potential energy at equilibrium. The physical interpretation of $\phi_\alpha(lk)$ is that it is the negative of the force acting in the α direction on a specific atom in the equilibrium configuration. However, in the equilibrium configuration the force on any particle must vanish, and so we have the result above in the equilibrium configuration.

The third term is quadratic and called the harmonic term, where a crystal is ideally considered as atoms connected by springs obeying Hooks law. Since this term is dominant, the anharmonic terms are taken to be just perturbations on the harmonic term. These perturbation terms are important in the study of heat transfer because they represent the major contribution to obtaining a finite thermal conductivity. If we consider the harmonic approximation, the Hamiltonian of the lattice vibrations can be written as:

$$H = \phi_0 + \frac{1}{2} \sum_{lk\alpha} M_k \dot{u}_\alpha^2(lk) + \frac{1}{2} \sum_{lk\alpha, l'k'\beta} \phi_{\alpha\beta}(lk, l'k') u_\beta(l'k') + ... \tag{2}$$

Where the second term is the kinetic energy, the other terms are taken from the Taylor expansion of the potential energy. α and β are the Cartesian coordinates.. The equation of motion can then be written as:

$$M_k \ddot{u}_\alpha(lk) = -\frac{\partial \phi}{\partial u_\alpha(lk)} \tag{3}$$

$$M_k \ddot{u}_\alpha(lk) = -\sum_{l'k'\beta} \phi_{\alpha\beta}(lk, l'k') u_\beta(l'k') \tag{4}$$

where $\phi_{\alpha\beta}(lk, l'k')$ is the second derivatives of potential energy with respect to displacement, evaluated at equilibrium. These terms will be related to elastic constants [25] The solution can be suggested based on the periodicity of the lattice:

$$u_\alpha(lk) = (M_k)^{-\frac{1}{2}} u_\alpha(k) exp[-iwt + i\mathbf{k}.\mathbf{x}(l)] \tag{5}$$

k is the wavevector and **x** is position vector. It can be noticed that due to periodicity u is independent of l. Substituting this solution in the equation of motion we find the dispersion relation, which is transformed to Fourier space.

$$w^2 u_\alpha(k) = \sum_{k'\beta} D_\alpha \beta(kk'|k) u_\beta(k') \tag{6}$$

Where the Fourier transformed dynamical matrix is such that:

$$D_{\alpha\beta}(kk'|\mathbf{k}) = (M_k M'_k)^{\frac{-1}{2}} \sum_{l'} \phi_{\alpha\beta}(lk; l'k') exp[-i\mathbf{k}.(\mathbf{x}(l) - \mathbf{x}(l'))] \tag{7}$$

Where M represents the corresponding atomic mass. The equation above reduces the problem from solving an infinite set of equations to solving $3r$ equations where r is the number of atoms. For the dynamical matrix to give a non-trivial solution we have:

$$|D_{\alpha\beta}(kk'|\mathbf{k}) - w^2 \delta_{\alpha\beta} \delta_{kk'}| = 0 \tag{8}$$

Which is an equation of degree 3r in w^2, there will be 3r solutions $w_j^2(k)$ for each value of $\mathbf{k}$, with j=1,2,..,3r. Now we make a coordinate transformation which simultaneously diagonalizes all the terms of the Hamiltonian. We generate the transformation by the wave expansion:

$$u_\alpha(lk) = (NM_k)^{\frac{-1}{2}} \sum_{kj} e_\alpha(k|\mathbf{k}j)Q(\mathbf{k}j)exp[i[\mathbf{k}.\mathbf{x}(l)]] \tag{9}$$

N is the number of lattices in the crystal and e is a vector of the solutions of the dispersion relation. The Hamiltonian then becomes:

$$H = \frac{1}{2}\sum_{\mathbf{k}j} \dot{Q}^*(\mathbf{k}j)\dot{Q}(\mathbf{k}j) + w_j^2(\mathbf{k})Q^*(\mathbf{k}j)Q(\mathbf{k}j) \tag{10}$$

The equation of motion will be:

$$\ddot{Q}(\mathbf{k}j) + w_j^2(\mathbf{k})Q(\mathbf{k}j) = 0 \tag{11}$$

Each of these normal coordinates is a periodic function of one of the frequencies $w_j(\mathbf{k})$. Hence they describe an independent crystal vibration mode of one frequency. The normal mode will be equal in number to the degrees of freedom in the crystal (3rN). Now, in order to describe $Q(\mathbf{k}j)$ in terms of real normal coordinates, we take:

$$Q(\mathbf{k}j) = \frac{1}{\sqrt{2}}[q_1(\mathbf{k}j) + iq_2(\mathbf{k}j)] \tag{12}$$

with q real. The Hamiltonian will become:

$$H = \frac{1}{2}\sum_{\mathbf{k}j} \dot{q^2}(\mathbf{k}j) + w_j^2(\mathbf{k})q^2(\mathbf{k}j) \tag{13}$$

Now substitute the property:

$$\dot{q}(\mathbf{k}j) = p(\mathbf{k}j) = -ih(\frac{\partial}{\partial q(\mathbf{k}j)}) \tag{14}$$

to finally obtain Schrodinger equation for lattice vibrations:

$$\frac{1}{2}\sum_{\mathbf{k}j}\left\{-\hbar^2\frac{\partial^2}{\partial q^2(\mathbf{k}j)}+w_j^2(\mathbf{k}j)q^2(\mathbf{k}j)\right\}\psi=E\psi \tag{15}$$

The wavefunction ψ is the product of the wavefunctions corresponding to each particle. (since H is the sum of independent particles). The total energy will also be the sum over all modes of energy:

$$E_n=\sum_{\mathbf{k}j}E_{nj}(\mathbf{k}) \tag{16}$$

The energy levels will have the form:

$$E_{nj}(\mathbf{k})=\big[n_j(\mathbf{k})+\frac{1}{2}\big]\hbar w_j(\mathbf{k}) \tag{17}$$

With $n_j(\mathbf{k})$ any integer.

Next, we define the momentum operator

$$P(\mathbf{k}j)=\dot{Q}(\mathbf{k}j) \tag{18}$$

And we will express Q and P in terms of the creation and annihilation operators defined by:

$$Q(\mathbf{k}j)=\big(\frac{\hbar}{2w_j(\mathbf{k})}\big)^{1/2}\big[a^+_{-\mathbf{k}j}+a_{\mathbf{k}j}\big] \tag{19}$$

The operators as usual obey the commutation relations:

$$[a_{\mathbf{k}j},a^+_{\mathbf{k}'j'}]=\triangle(\mathbf{k}-\mathbf{k}')\delta_{jj'} \tag{20}$$

$$[a_{\mathbf{k}j},a_{\mathbf{k}'j'}]=[a^+_{\mathbf{k}j},a^+_{\mathbf{k}'j'}]=0 \tag{21}$$

By this transformation, the Hamiltonian takes the simple form:

$$H = \sum_{\mathbf{k}j} \hbar w_j(\mathbf{k})[a^+_{\mathbf{k}j}, a_{\mathbf{k}'j'} + \frac{1}{2}] \tag{22}$$

Knowing that the creation and annihilation operators commute then we deduce that all Hamiltonians of particles can be simultaneously diagonalized. The creation operator will increase the number of phonons in a known state by one, whereas the destruction operator decreases the phonons by one. It can be also seen that the energy levels of the lattice vibrations are equally spaced by an energy difference $\hbar w$. The above derivation was made for the harmonic approximation of H. However we can make a transformation for the anharmonic perturbation by similar steps, and we obtain:

$$\begin{aligned} H^{(3)} = \frac{1}{3!} \sum_{\mathbf{k}\mathbf{k}'\mathbf{k}'', jj'j''} & \delta_{G,\mathbf{k}+\mathbf{k}'+\mathbf{k}''} V_{(3)}(\mathbf{k}j, \mathbf{k}'j', \mathbf{k}''j'') \\ & \times (a^+_{\mathbf{k}j} - a_{-\mathbf{k}j})(a^+_{\mathbf{k}'j'} - a_{-\mathbf{k}'j'})(a^+_{\mathbf{k}''j''} - a_{-\mathbf{k}''j''}) \end{aligned} \tag{23}$$

$V_{(3)}$ is the cubic anharmonicity coefficient. We notice that the anharmonic term is not diagonalized which is expected by the nature of anharmonicity which makes a connection between oscillators which were taken to be independent by the harmonic study. Physically, the description of phonons number and energy is obtained by the harmonic study while the phonons interactions are derived from the anharmonic term.

B. The Contribution of Each High-Symmetry Direction to the Total Thermal Conductivity

Finally, after studying phonon propagation in the crystal, one can describe thermal conductivity using the properties of these heat carriers.

Initially, thermal conductivity is defined as the ratio of heat current density over the

temperature gradient.

$$\kappa(T) = \frac{-1}{A}\frac{J_Q}{\nabla T} \tag{24}$$

summing over all phonon wavevectors and polarizations,

$$\kappa(T) = \sum_j \sum_k \hbar w_j(k) \tilde{N}_{j,k} \frac{v_{j,k}}{\nabla T} \tag{25}$$

where $w_j(k) \quad and \quad v_{j,k}$ are phonon frequency and group velocity corresponding to wavevector k and polarization j, and $\tilde{N}_{j,k}$ is the deviation of the phonon distribution from equilibrium in the state k. $\tilde{N}_{j,k}$ is defined as the difference between the phonon distribution out of equilibrium $N_{j,k}$ and the Plank phonon distribution at equilibrium $\bar{N}_{j,k}$.

In order to evaluate $\kappa(T)$, it is more convenient to deal with the frequency distribution function with the sum over these modes. The total frequency distribution function is defined as

$$g(w) = \left(\frac{2w}{3rN_c} \sum_j \sum_k \delta(w^2 - w_j^2(k)) \right) \tag{26}$$

where r is the number of atoms per unit-cell and N_c is the number of cells in the crystal. It follows that the frequency distribution function of the j^{th} phonon branch can be expressed as

$$g_j(w) = \left(\frac{2w}{3r(2\pi)^3} \right) v_B^{-1} \int \delta\left(w^2 - w_j^2(k)\right) d^3k \tag{27}$$

where v_B is the volume of the first Brillouin zone, $w_j(k)$ are the roots of the distribution function and the integral is carried out through the first Brillouin zone. Now, if we change to spherical polar coordinates (k, θ, ϕ), and use the relation

$$\delta(f(x)) = \sum_i \frac{\delta(x - x_i)}{|f'(x_i)|} \tag{28}$$

where x_i are simple zeros of $f(x)$, Equation 28 is transformed into

$$g_j(w) = \frac{1}{3r(2\pi)^3 v_B} \int_0^{\pi} sin\theta d\theta \int_0^{2\pi} d\phi k_j^2(w,\theta,\phi) \frac{dk_j(w,\theta,\phi)}{dw} \tag{29}$$

where $k_j(w,\theta,\phi)$ is the solution to $w = w_j(k,\theta,\phi)$. This means that the quantity $\frac{1}{3r(2\pi)^3 v_B} k_j^2(w,\theta,\phi) dk_j(w,\theta,\phi)$ is the frequency distribution function per unit solid angle for the j^{th} branch of the total phonon spectrum. Let us denote this quantity by $g_j(w,\theta,\phi)$. The idea behind this transformation is as follows. The function $g_j(w,\theta,\phi)$ has cubic symmetry in θ and ϕ because the normal mode frequencies are invariant against any real orthogonal transformation of axes which takes the crystal to itself. This means that $g_j(w,\theta,\phi)$ can be expanded in terms of cubic harmonics, K_m , which have the symmetry of the lattice,

$$g_j(w,\theta,\phi) = \sum_{m=0}^{\infty}{}' a'_m(w) K_m(\theta,\phi) \tag{30}$$

where $K_0 = 1$ and the prime on the summation means that the term corresponding to $m = 1$ is to be omitted from the summation. The K_m terms satisfy the orthogonality condition

$$\int_0^{\pi} sin\theta d\theta \int_0^{2\pi} d\phi K_m(\theta,\phi) K_n(\theta,\phi) = 4\pi\gamma_m \delta_{mn} \tag{31}$$

where γ_m is a normalization constant and δ_{mn} is the usual Kronecker symbol. The method for generating γ_m and the cubic harmonics are reported in reference [26]. The first three γ_m are $\gamma_0 = 1, \gamma_1 = 0, \gamma_2 = \frac{16}{3.5.5.7}$, and the first three cubic harmonics are $K_0 = 1, K_1 = 0, K_2 = x^4 + y^4 + z^4 - 3/5\rho^4$, where $\rho^2 = x^2 + y^2 + z^2$. Now, if we substitute Equation 30 into Equation 29 and make use of Equation 31, we obtain

$$g_j(w) = 4\pi a_0(w) \tag{32}$$

The coefficient $a_0(w)$ can be obtained by following Huston's procedures. It can be considered that there exist directions in reciprocal space along which the cubic crys-

tal dynamical matrix factors into equations of low degree in w^2 which can be solved exactly for w as a function of the wavevector k. These directions are high symmetry directions such as (100), (110), and (111) directions. Along these directions the equation $w = w_j(k, \theta, \phi)$ can be expressed as $w = w_j(k_s, \theta_s, \phi_s)$. Since these equations can be inverted exactly to obtain for simple enough models, it follows that $g_j(w_s, \theta_s, \phi_s)$ can be exactly obtained for these special directions. If we then retain as many terms in Equation 30 as the number of directions (θ_s, ϕ_s), the $a_m(w)$ in Equation 30 are given as the solution of a set of simultaneous linear equations whose coefficients are the values of $g_j(w, \theta, \phi)$ along the direction (θ_s, ϕ_s). In particular, it follows from Equation 30, 31, and 32 that the total frequency distribution function for the j^{th} branch can be expressed in terms of the frequency distribution functions along the (100), (110), and (111) directions (which in principal can be obtained with satisfactory accuracy)

$$g_j(w) = \frac{4\pi}{35}\left[10.g_j^{(A)}(w) + 16g_j^{(B)}(w) + 9g_j^{(C)}(w)\right] \tag{33}$$

where the superscripts A, B, and C on g signify (100), (110), and (111) respectively. The evaluation of $g_j^{(A)}$, $g_j^{(B)}$ and $g_j^{(C)}(w)$ can be simplified by noting that Huston's method illustrated above can be used for the approximate evaluation of any integral of the form

$$J = \int_0^{\pi} sin\theta d\theta \int_0^{2\pi} d\phi I(\theta, \phi) \tag{34}$$

provided that $I(\theta, \phi)$ has cubic symmetry. In fact, from the general form of a three-dimensional dynamical matrix one can find that the leading term in the expansion of $w_j^2(\mathbf{k})$ is of $O(k^2)$, and since the long wavelength acoustic phonons have the major contribution to the lattice thermal conductivity, we can consider only small values of k. In that limit, we must have

$$w_j^2(\mathbf{k}) = C_j^2(\theta, \phi)k^2 + D_j^2(\theta, \phi)k^4 + ... \tag{35}$$

where the coefficients C_j and D_j have the symmetry of the lattice. Upon inverting Equation 35, we find the frequency distribution function per unit solid angle for the j^{th} branch of the spectrum

$$g_j(w,\theta,\phi) = \frac{1}{3rv_B}\frac{1}{(2\pi)^3}\left[\frac{w^2}{C_j^3(\theta,\phi)} - \frac{5}{2}\frac{D_j^2(\theta,\phi)}{C_j^7(\theta,\phi)}w^4 + ...\right] \tag{36}$$

On the other hand, for small values of w , the phonon spectrum of a three-dimensional crystal has the expansion

$$g(w) = a_2w^2 + a_4w^4 + ... \tag{37}$$

Thus, from Equation 29, Equation 36, and Equation 37 we find that

$$a_2 = \frac{1}{3rv_B}\frac{1}{(2\pi)^3}\sum_j\int_0^{\pi}\int_0^{2\pi}\frac{sin\theta d\theta d\phi}{C_j^3(\theta,\phi)} \tag{38}$$

and

$$a_4 = -\frac{5}{2}\frac{1}{3rv_a}\frac{1}{(2\pi)^3}\sum_j\int_0^{\pi}\int_0^{2\pi}\frac{D_j^2(\theta,\phi)sin\theta d\theta d\phi}{C_j^7(\theta,\phi)} \tag{39}$$

It is clear from Equation 35 that the coefficients $C_j(\theta,\phi)$ are the phonon group velocities for a given direction (θ,ϕ) of propagation. Thus, by applying Huston's method to the evaluation of the integral in Equation 38, we find that the coefficients of the low frequency end of the phonon spectrum can be expressed in terms of directional phonon group velocities as

$$a_2 = \frac{1}{3rv_B}\frac{1}{(2\pi)^3}\frac{4\pi}{35}\sum_j\left[\frac{10}{v_{j(100)}^3}\frac{16}{v_{j(110)}^3} + \frac{9}{v_{j(111)}^3}\right] \tag{40}$$

where $j(hkl)$ is the group velocity of the phonon of the j^{th} branch along the high-symmetry direction $[hkl]$. Hence, in view of Equation 37, and assuming a Debye-

like dispersion relations, the phonon spectrum can be approximated by

$$g(w) = \frac{1}{3rv_s}\frac{1}{(2\pi)^3}\frac{4\pi}{35}\sum_j \left[\frac{10}{v^3_{j(100)}}\frac{16}{v^3_{j(110)}} + \frac{9}{v^3_{j(111)}}\right]w^2 \tag{41}$$

The total phonon frequency distribution function g(w) can thus be approximated by the sum of three terms, and each term is a function of the frequency distribution in a high-symmetry direction. In view of Equation 24, Equation 40, and Equation 41, we can express the lattice thermal conductivity as

$$\begin{aligned}\kappa(T) = \frac{1}{rv_B\pi^2}\sum_j \Bigg[&\frac{1}{21}\int_0^{w_{D,j(100)}} \hbar w_j(k)\tilde{N}_{j,k_{100}}\frac{v_{j(100)}}{|\nabla T|}cos\psi_{100}\frac{w_j^2(k)}{v^3_{j(100)}}dw \\ &+\frac{8}{105}\int_0^{w_{D,j(110)}} \hbar w_j(k)\tilde{N}_{j,k_{110}}\frac{v_{j(110)}}{|\nabla T|}cos\psi_{110}\frac{w_j^2(k)}{v^3_{j(110)}}dw \\ &+\frac{3}{70}\int_0^{w_{D,j(111)}} \hbar w_j(k)\tilde{N}_{j,k_{111}}\frac{v_{j(111)}}{|\nabla T|}cos\psi_{111}\frac{w_j^2(k)}{v^3_{j(111)}}dw\Bigg]\end{aligned} \tag{42}$$

where the integrals upper limits $w_{D,j(hkl)}$ are artificial limiting frequencies leading to correct normalization of $g_j^{(A)}(w)$, $g_j^{(B)}(w)$ and $g_j^{(C)}(w)$. k_{hkl} denotes a wavevector in high-symmetry direction [hkl], and ψ_{hkl} is the angle between the high-symmetry direction [hkl] and the temperature gradient.

C. Evaluation of the Deviation of the Phonon Distribution Function From Spatial-Dependent Boltzmann Equation

After obtaining the final formula for the thermal conductivity as a function of high-symmetry weights of the frequency distribution we need to evaluate the different parameters of the formula. In order to evaluate the displaced phonon distribution function, the Boltzmann equation is used for the classical study of phonons since we are studying the atomic vibrations which are described by Bose-Einstein's distribution, knowing that phonons are Bosons. The Boltzmann equation describes the total rate of change in the phonon distribution due to a disturbance by a temperature

gradient. The expression of thermal conductivity will be derived from the solution of this equation.

At equilibrium, $\bar{N} = \frac{1}{exp(\frac{hw}{K_B T})-1}$. Due to a temperature gradient applied to bulk crystals, the phonon distribution function diverges from its equilibrium value. Boltzmann's equation describes the change in the distribution function in this case by:

$$-v.\nabla N + \frac{\partial N}{\partial t} = 0 \tag{43}$$

v is the speed of sound in the crystal. The first term in the equation represents the variation in number of modes due to temperature gradient while the second term gives the variation due to different phonon modes.

The first term can be written as :

$$v.\nabla N = v.\nabla T \frac{dN}{dT} \tag{44}$$

In the second term, using the relaxation time approximation provided by Callaway [27], and knowing that phonon processes are two types, normal processes (which tend to deviate phonons from equilibrium) and resistive processes (which tend to bring the deviation back to equilibrium), we get an expression for the second term.

$$(\frac{\partial N}{\partial t})_c = \frac{\tilde{N} - N}{\tau_N} + \frac{\bar{N} - N}{\tau_{u+I}} \tag{45}$$

$\bar{N}$ is the phonon distribution function at equilibrium, N is the phonon distribution at a given q, and

$$\tilde{N} = \left[exp(\frac{hw - \lambda.k}{K_B.T}) \right]^{-1} \tag{46}$$

is the displaced phonon distribution, which is stationary in the state k_{hkl} for the normal processes, τ_N is the relaxation time for normal processes while τ_R is the relaxation time for resistive processes. The relaxation time associated with the

resistive processes is defined by:

$$\tau_{U+I}^{-1} = \tau_U^{-1} + \tau_I^{-1} \tag{47}$$

where $\tau_U^{-1} \quad and \quad \tau_I^{-1}$ are relaxation times associated with Umklapp processes and phonon scattering by localized mass-difference. Klemen's theory can be used to calculate τ_I^{-1}, and the conventional Fermi's golden rule formula based on the cubic harmonic part of the crystal Hamiltonian as perturbation can be used to calculate $\tau_N^{-1} \quad and \quad \tau_U^{-1}$. With this approximation the difference between the physical nature of the phonon normal processes, which tend to displace the phonon distribution function, and that of the resistive processes, which tend to restore the distribution function back to its equilibrium value is taken into account. Now, if we consider a finite crystal (a crystal with borders) in which the resistive processes dominate the normal ones, and if we assume that the temperature gradient is along the z-direction and too weak to significantly displace the distribution function and have effect in the x and y directions, the spatial-dependent Boltzmann equation describing the rate of change in the phonon distribution takes the form:

$$v_z \frac{d\tilde{N}}{dT}\frac{\partial T}{\partial z} + v_x \frac{\partial \tilde{N}}{\partial x} + v_y \frac{\partial \tilde{N}}{\partial y} + \frac{\tilde{N}}{\tau} = 0 \tag{48}$$

With that form of Boltzmann equation it can be seen that the phonon distribution function has an explicit x and y dependence, with an implicit dependence on z through the temperature gradient. The solution of Equation 48 can be found if we realize that in the very vicinity of the sample border, parallel to the heat current, phonons are either at thermal equilibrium with the border or out of equilibrium due to interaction with surface phonons. At the opposite border, all the phonons of wavevector k are absorbed then re-emitted or reflected with momentum and equilibrium distribution. With these considerations, the solution of Equation 48 takes

the form

$$\tilde{N} = \frac{R\tau_U}{2}\left[\left(1 - exp(\frac{-x(y)}{\tau_{U+I}v_x})\right) + \left(1 - exp(\frac{-y(x)}{\tau_{U+I}v_y})\right)\right] + \sigma_z exp(\frac{-x(y)}{\tau_{U+I}v_x}) + \sigma_z exp(\frac{-y(x)}{\tau_{U+I}v_y}) \tag{49}$$

where R is given by the negative of phonons rate per unit volume of reciprocal space:

$$R = -v_z \frac{d\bar{N}}{dT}\frac{\partial T}{\partial z} \tag{50}$$

x(y) is the y-dependent distance from the boundary parallel to the x-axis and y(x) is the x-dependent distance from the boundary parallel to the y-axis. both distances are measured perpendicular to the direction of the temperature gradient. σ_z is the phonon distribution deviation by surface phonons due to interactions with phonons in the volume.

Now, substituting this solution in the Boltzmann equation obtained before, we get:

$$R = -(\frac{1}{\tau_{B,x}} + \frac{1}{\tau_{B,y}} + \frac{1}{\tau})\langle\tilde{N}\rangle \tag{51}$$

where

$$\frac{1}{\tau_{\beta,\alpha}} = \frac{\int_\alpha \frac{\partial\tilde{N}}{\partial\alpha}dxdy}{\int\int\tilde{N}dxdy} \tag{52}$$

$\alpha = x, y$ and

$$\langle\tilde{N}\rangle = \frac{\int\int\tilde{N}dxdy}{\int\int dxdy} \tag{53}$$

Thus, the effect of the samples borders is to add resistance to the phonons. The rate at which the phonons scatter by the borders can be found by substituting Equation 49 in Equation 52, and noting that the term $\frac{2\sigma_z}{\tau_{U+I}R}$ that appears in the resulting equation is nothing but the specularity factor, which is usually approximated by $P = exp(\frac{-16\pi^2h^2w^2}{v^2})$, where h is the root mean square (rms) roughness at the sample borders. The advantage of Equation 52 on Casimir formula, which is widely used

to evaluate the phonon-boundary scattering rate, is that it describes the rate at which phonons are scattered by the sample borders in the presence of intrinsic scattering processes. The boundary scattering rate expressed in equation 52 decreases as the intrinsic scattering rate increases. This can be fully understood if we realize that when the intrinsic scattering increases the probability that the phonons reach the sample borders decreases, so the phonon-boundary scattering rate decreases.Such interplay between phonon intrinsic scattering and phonon-boundary scattering is not taken into account with the conventional Casimir theory. Hence, for finite crystals, the original Boltzmann equation takes the form

$$v_z \frac{d\bar{N}}{dT}\frac{\partial T}{\partial z} + \frac{N_u - N}{\tau_N} + \frac{\bar{N} - N}{\tau_R} = 0 \tag{54}$$

where $\frac{1}{\tau_R} = \frac{1}{\tau_{B,x}} + \frac{1}{\tau_{B,y}} + \frac{1}{\tau_I} + \frac{1}{\tau_U}$ is the overall resistive scattering rate. The displaced Plank distribution for a random crystallographic direction $[hkl]$ is defined as

$$N_u = \bar{N} + \frac{\mathbf{u}_{[hkl]}\mathbf{k}_z}{k_B T}\frac{exp(\frac{\hbar w}{k_B T})}{(exp(\frac{\hbar w}{k_B T}) - 1)^2} \tag{55}$$

where $\mathbf{k}_z$ is a wavevector in the z-direction. Upon using Equation 55 in Equation 54, the original Boltzmann equation takes the form

$$\frac{\hbar w}{k_B T^2}\frac{exp(\frac{\hbar w}{k_B T})}{(exp(\frac{\hbar w}{k_B T}) - 1)^2} v_Z \frac{\partial T}{\partial z} + \frac{\mathbf{u}_{[hkl]}\mathbf{k}_z}{k_B T \tau_N}\frac{exp(\frac{\hbar w}{k_B T})}{(exp(\frac{\hbar w}{k_B T}) - 1)^2} - \tilde{N}(\frac{1}{\tau_N} + \frac{1}{\tau_R}) = 0 \tag{56}$$

Following the reasoning by Callaway, we introduce a combined relaxation time τ_C defined as

$$\frac{1}{\tau_C} = \frac{1}{\tau_N} + \frac{1}{\tau_R} \tag{57}$$

and express $\tilde{N}$ as

$$_u = N - \bar{N} = \alpha(k) v_z \frac{\partial T}{\partial z}\frac{\hbar w}{k_B T^2}\frac{exp(\frac{\hbar w}{k_B T})}{(exp(\frac{\hbar w}{k_B T}) - 1)^2} \tag{58}$$

where $\alpha(k)$ has the dimension of time. Upon substituting Equation 58 in Equation 56 we find

$$-\frac{\hbar w}{T\tau_C}\alpha(k)v_z\frac{\partial T}{\partial z}+\frac{\mathbf{u}_{[hkl]}\mathbf{k}_z}{\tau_N}=-\frac{\hbar w}{T}v_z\frac{\partial T}{\partial z} \tag{59}$$

Since $\mathbf{u}_{[hkl]}$ is a vector that has the dimension of energy times length and points in the direction of the temperature gradient (z-direction), we can express it as

$$\mathbf{u}_{[hkl]}=\frac{\hbar}{T}\beta_{[hkl]}v_z^2\frac{\partial T}{\partial z}\hat{\mathbf{z}} \tag{60}$$

where $\hat{\mathbf{z}}$ is a unit vector in the z-direction and $\beta_{[hkl]}$ is a parameter having the dimension of a relaxation time. It follows that within the approximation of linearised dispersion relations, i.e., $\mathbf{k}_z=\frac{w}{v_z}\hat{\mathbf{z}}$, Equation 59 reduces to

$$\alpha(k)=\tau_C(1+\frac{\beta_{[hkl]}}{\tau_N}) \tag{61}$$

To find $\beta_{[hk]}$ in the high-symmetry directions, we can take advantage of the fact that the normal processes conserve the total crystal momentum. This can be expressed as

$$\sum_j\sum_k\left(\frac{\partial N}{\partial t}\right)_N\mathbf{k}=\sum_j\sum_k\frac{N_u-N}{\tau_N}\mathbf{k}=0 \tag{62}$$

upon using equations 55-58 and $\mathbf{k}_z=\frac{w}{v_z}\hat{\mathbf{z}}$ in Equation 62 we find

$$\sum_j\sum_k\frac{exp(\frac{\hbar w}{k_BT})}{(exp(\frac{\hbar w}{k_BT})-1)^2}\frac{\hbar w}{k_BT^2}(\alpha(k)-\beta_{[hkl]})\frac{\mathbf{k}}{\tau_N}=0 \tag{63}$$

The use of the phonon spectrum expressed in Equation 41 allows writing Equation

63 in the form

$$\sum_j \left[\frac{1}{21} \int_0^{w_{D,j(100)}} \frac{exp\left(\frac{\hbar w}{k_B T}\right)}{\left(exp\left(\frac{\hbar w}{k_B T}\right)-1\right)^2} \frac{\hbar w^4}{k_B T^2 v_{j(100)}^4} (\alpha(k_{100}) - \beta_{[100]}) \frac{1}{\tau_{N,(100)}} dw \hat{\mathbf{i}}_{100} \right.$$
$$+ \frac{8}{105} \int_0^{w_{D,j(110)}} \frac{exp\left(\frac{\hbar w}{k_B T}\right)}{\left(exp\left(\frac{\hbar w}{k_B T}\right)-1\right)^2} \frac{\hbar w^4}{k_B T^2 v_{j(110)}^4} \left(\alpha(k_{110}) - \beta_{[110]}\right) \frac{1}{\tau_{N,(110)}} dw \hat{\mathbf{i}}_{110}$$
$$\left. + \frac{3}{70} \int_0^{w_{D,j(111)}} \frac{exp\left(\frac{\hbar w}{k_B T}\right)}{\left(exp\left(\frac{\hbar w}{k_B T}\right)-1\right)^2} \frac{\hbar w^4}{k_B T^2 v_{j(111)}^4} \left(\alpha(k_{111}) - \beta_{[111]}\right) \frac{1}{\tau_{N,(111)}} dw \hat{\mathbf{i}}_{111} \right] = 0 \tag{64}$$

where $\hat{\mathbf{i}}_{hkl}$ is a unit vector in the direction, $\tau_{N,(hkl)}$ is the relaxation time associated with the normal processes of the modes in the $[hkl]$ direction, $\alpha(k_{hkl})$ is the relaxation time defined in Equation 58 for the wavevectors in the $[hkl]$ direction, and $\beta_{[hkl]}$ is the relaxation time defined in Equation 60 for the $[hkl]$ direction. Since the vector $\mathbf{u}_{[hkl]}$ defined in Equation 60 is a constant vector in the $[hkl]$ direction, should be independent of the frequency in the direction. This allows using Equation 64 to evaluate for the high-symmetry directions of a cubic crystal. Since we consider that the temperature gradient is along the z-direction and has no effect in the other directions, the obtained form of $\kappa(T)$ is

$$\kappa(T) = \frac{1}{\Omega} \frac{v_z k_B}{r v_B \pi^2} \left(\frac{k_B T}{\hbar}\right)^3 \sum_j \sum_{[hkl]} \chi \frac{cos\psi_{hkl}}{v_j^2(hkl)} \left[\int_0^{\theta_{D,l(hkl)/T}} \tau_{C,j(hkl)} x^4 \frac{exp(x)}{(exp(x)-1)^2} dx \right.$$
$$\left. + \beta_{[hkl]} \int_0^{\theta_{D,l(hkl)/T}} \frac{\tau_{C,j(hkl)}}{\tau_{N,j(hkl)}} \tau_{C,j(hkl)} x^4 \frac{exp(x)}{(exp(x)-1)^2} dx \right] \tag{65}$$

where the summation $\sum_{[hkl]}$ runs over all the high-symmetry directions, $\chi_{100} = 1/21, \quad \chi_{110} = 8/105, \quad \chi_{111} = 3/70$ and v_z is the phonon group velocity in the direction of the temperature gradient averaged over all phonon polarizations. At this point, we are able to weigh the contribution of each phonon mode to the thermal conductivity along all directions and account for the effects of the material

shape and size on the thermal conductivity.

D. Calculating Relaxation Times of Phonon Processes

An important variable in the Boltzmann equation is the relaxation time of phonon scattering processes. As phonons propagate throughout the lattice, they undergo various physical processes which might alter their propagation. The scattering processes are the reason behind obtaining a finite thermal conductivity. Otherwise phonons would propagate infinitely throughout the crystal and will be transporting heat perfectly from side to side because their propagation is uniform. The scattering of phonons can be due to colliding with other propagating phonons, reaching a boundary, or colliding to structural obstacles such as impurities or atomic dislocations... To account for these scatterings which limit the thermal conductivity, we study the different relaxation times of these processes. Phonon relaxation times represent the time through which a phonon propagates before it scatters due to a certain phonon process. In this section, a description of different phonon processes is presented as well as the relaxation time for each phonon process.

1. Relaxation Time for Three-Phonon Scattering

The study of phonon modes and their properties briefed earlier were based on the assumption that phonons interacted harmonically. However, in this idealization, there will be no resistance to heat flow and the result will be an infinite thermal conductivity for any perturbation. Trivially, measurements show limited thermal conductivity that varies with different properties which affect the phonon scattering processes inside the crystal through their propagation. Hence accounting for anharmonic terms is required to demonstrate correct thermal conductivity calculations.

The main process contributing to phonon scattering is the phonon- phonon scat-

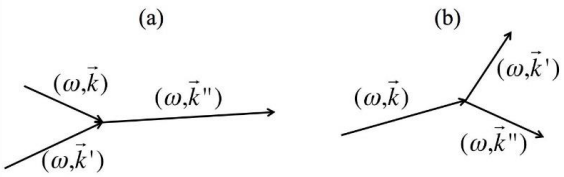

Figure 3: (a) An inelastic phonon-phonon scattering corresponding to phonon annihilation, and (b) Inelastic phonon-phonon scattering by creation[7]

tering due to anharmonic interactions between phonons. The anharmonic interaction results from the third term in the expanded interatomic potential which was neglected in the harmonic approximation. This term is now considered as a perturbation on the Hamiltonian derived for the harmonic modes. Using Fermi's golden rule, it was shown by Ziman that the anharmonic term acted on phonons either by creation or by annihilation mechanisms [28]. These scattering processes are known as three-phonon scatterings. In Figure 3, the three-phonon scattering modes are presented, where scattering either causes two phonons to merge into one phonon of higher energy or one phonon to split into two phonons of lower energy.

In the case of phonon annihilation, conservation of phonon energy gives:

$$h\nu_1 + h\nu_2 = h\nu_3 \tag{66}$$

While momentum conservation has a special formula,

$$k_1 + k_2 + k_3 = G \tag{67}$$

If the emerging phonon falls inside the Brillouin zone, the reciprocal lattice vector G will be zero. But if the emerging phonon is outside the Brillouin zone, then G will be non-zero so as it returns the emerging phonon back into the Brillouin Zone so that the phonon wavelength remains greater than the lattice constant. Figure 4 shows the two types of three-phonon scatterings: If $G = 0$, the scattering process will be called the normal scattering process, where the emerging phonon(s) will

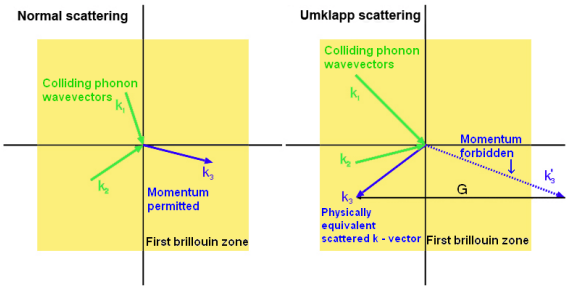

Figure 4: three-phonon scattering processes

preserve the energy and direction of the scattered phonon(s), thus favouring thermal conductivity in the lattice. On the other hand, for $G \neq 0$, the scattering process will be known as the resistive phonon scattering, where the non-zero reciprocal lattice vector will change the phonon propagation direction and thus the emergent phonon will resist heat conduction across the lattice by producing an opposing flow.

Due to the energy selection rules, it is expected that two acoustic phonons can merge to create an optical phonon, while two optical phonons can't form an acoustic phonon. Similarly, an acoustic phonon can merge with an optical phonon and give an optical phonon but can't give an acoustic phonon because it has a lower energy than the sum of the two annihilated phonons' energies. The lifetime of phonon scattering is essential for calculating the thermal conductivity of the crystal, this relaxation time can give the mean free path which is the distance a phonon would travel before it undergoes scattering. Evaluating the relaxation time due to three-phonon scattering was derived by approximations of scattering integrals by Klemens in 1958, and the formula obtained had the form:

$$\tau_{N,L}^{-1} = B_{N,L} w^2 T^3 \tag{68}$$

for longitudinal phonons, and:

$$\tau_{N,T}^{-1} = B_{N,T} w T^4 \tag{69}$$

for transverse phonons. Where B is a constant obtained from comparing with experimental measurements, and θ_D is the Debye temperature. For resistive processes, the relaxation time will have the form:

$$\tau_{u,L}^{-1} = B_{u,L} w^2 T exp(\frac{-\theta_{D,L}}{3T}) \tag{70}$$

for longitudinal phonons, and:

$$\tau_{U,T}^{-1} = B_{U,T} w^2 T exp(\frac{-\theta_{D,T}}{3T}) \tag{71}$$

for transverse phonons.

2. Relaxation Time Due to Phonon Point Defect Scattering

The isotopic composition of a crystal affects the phonon transport since the isotopes are observed by phonons as point defects on which they scatter. Analytical expressions for the relaxation time can be obtained from a model presenting point defects in a perfect lattice [10] . The obtained expression by Klemens depends on the branch under study:

$$\tau_{I,j}^{-1} = \frac{V\sigma}{4\pi v^3} w^4 \tag{72}$$

V is the volume per atom σ is a parameter describing the mass fluctuation-phonon scattering:

$$\sigma = \frac{\sum_i (c_i M_i)^2 - (\sum_i c_i M_i)^2}{(\sum_i c_i M_i)^2} \tag{73}$$

c_i represents the concentration of the isotope M_i represents the mass of the isotope.

3. Effect of Alloys

The thermal conductivity of a single crystal alloy is found to be lower than the average thermal conductivity of the constituent material of this alloy. To obtain relaxation time for scattering by the alloys we consider that the crystal virtually has ordered alloys, and the actual disorder in alloys is considered a perturbation [29]. An average atomic weight of this crystal will have the form $\bar{M} = \sum_i f_i M_i$ where M_i and f_i are the atomic mass and concentration of the i^{th} component of the alloy. Then similar to the process of impurity scattering, we consider that an atom of the virtual crystal is replaced by an atom from the alloy, which then becomes a virtual impurity of mass defect $\triangle M_i = M_i - \bar{M}$. Since virtual impurities have different masses, then different coupling forces exist at this location and phonons will then undergo scattering. By similar treatment to point defect scattering, the obtained relaxation time will be proportional to w^4.

E. Experimental Measurements of Thermal Conductivity

Measurements of thermal conductivity in crystals showed a general trend as shown in figure5. At low temperatures, thermal conductivity increases with temperature in a cubic form, and through this region heat transfer is highly dependent on lattice size and shape. Then a maximum of thermal conductivity is obtained at $T = 0.05\theta_D$ where heat transfer is dependent on isotopic composition and sensitive to imperfections. Afterwards, thermal conductivity decreases due to the increase of scattering by normal processes. When the temperature becomes more than $0.1\theta_D$, thermal conductivity decreases due to Umklapp processes.

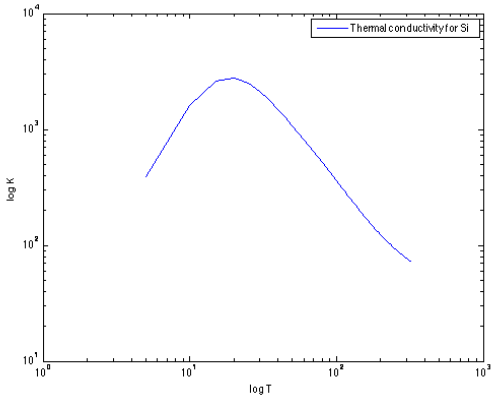

Figure 5: thermal conductivity of Bulk Silicon as a Function of Temperature.[30]

F. Suggested Model with Temperature Dependent Vibrational Parameters

Although they give somewhat reasonable fit to the experimental data, all previously developed models involve free adjustable parameters. Consequently, they can be used somehow as analysis models but not as predictive models for the lattice thermal conductivity. Using the solution obtained from the Boltzmann equation, together with approximate lattice dynamical matrix, this section will provide a predictive model for the lattice thermal conductivity with temperature dependent parameters related to the lattice dynamics. The result will be a full description of thermal conductivity in semiconductors without any fitting parameters. Velocity of sound in the crystal is weighty in the calculation of thermal conductivity as it appears in the expression giving the heat current density, in the constants multiplying the relaxation times as well as in the calculation of heat capacity. In our model, sound velocity values were obtained from their dependence on elastic constants and density of the material that stems from Green-Christoffel equation in elasticity theory which is valid for small wave vectors. Assuming that the theory works within the temperature range that we are considering in our work, $T < 400k$, we calculate sound velocity from Green-Christoffel equation. In principle, the developed model can account for the thermal conductivity of finite crystals of any geometrical shape. However, we will consider here the simple case of a finite three-dimensional crystal

having the shape of a parallelepiped of dimensions l_1, l_2 and l_3. If we consider the crystal as a continuum medium and ignore interference effects between incident and reflected acoustic waves, the acoustic phonon dispersion relations can be written as

$$\rho w^2 u_\alpha^{(0)} = \sum_\beta \sum_{\gamma\lambda} c_{\alpha\gamma\beta\lambda} k_\gamma k_\lambda u_\beta^{(0)} \tag{74}$$

where ρ is the density of the crystal, $c_{\alpha\gamma\beta\lambda}$ are the elements of the $(6x6)$ matrix where the subscripts correspond to the coordinates, w is the frequency of vibrations of the crystal and u_α is the displacement vector. k_α and k_λ are the components of the wave vectors along the direction under consideration. For the two sides of equation 74 to be equal for any vector u_α, the determinant of the following matrix should be set to zero:

$$|Iw^2(k) - A_{\alpha\beta}(k)| = 0 \tag{75}$$

where

$$A_{\alpha\beta} = \frac{1}{\rho} \sum_{\gamma\lambda} c_{\alpha\gamma\beta\lambda} k_\lambda (76)$$

For a given frequency we can get the velocity of the phonon of a known wavevector, with the assumption of a linear dispersion relation. Sound velocity will be variable with respect to the direction of the propagation of phonons in the crystal, waves propagating along [001] direction will have sound velocity that differs if the waves were along [110] direction. Equation 75 is cubic in v^2 and the result will be three roots that correspond to one longitudinal and two transverse phonons. Generally, the three of them are all distinct. Previous models which proposed a theoretical calculation of thermal conductivity for bulk materials assumed a constant Debye temperature and Gruneisen parameter. We mentioned that actually, these two parameters depend appreciably on temperature. With this dependence taken into account, the range of temperature within which our model works accurately would be extended.

1. Temperature Dependent Specific Heat

Typically, if we compare the exact frequency spectrum of a given material with the corresponding linear spectrum, we see that they coincide up to a frequency such that $\hbar w = 0.1 k_B \theta_D^{(0)}$ where $\theta_D^{(0)}$ is material Debye temperature at $0K$. Moreover, the Debye temperature remains constants only for a few degrees above $0K$ [5] [31]. Therefore, the consideration of a linear spectrum approximation with a constant Debye temperature can accurately describe the temperature dependence of phonon related properties only in the temperature range.

In the Debye approximation, the velocity of sound is taken to be constant for each phonon mode. The phonon dispersion relation is taken to be linearly dependent on the phonon wave vector, where the speed of sound is the proportionality constant: w = ck. This assumption works well near the center of the Brillouin zone, for small k, and may deviate on the edges. If N is the number of primitive cells in a given specimen, then we expect to have N acoustic phonon modes. A cut off frequency is thus set by the maximum number of modes. This maximum frequency defines a characteristic temperature known as the Debye temperature which determines the temperature of the highest normal mode of vibration. Debye temperature is a main parameter in our calculations. Relaxation time of Umklapp processes depends directly on the Debye temperature through its constant. It also sets the integration limit of all the integrals involved in calculating k(T). Debye temperature is always assumed to be a constant, an approximation which is not valid since reported experimental measurements of θ_D revealed a strong dependence on temperature[6].

In order to be able to compute θ_D as a function of temperature, we need to start from modelling phonons in a crystal by quantum oscillators. In a crystal containing N atoms, there are $3N$ springs. The Hamiltonian corresponding to the problem of a vibrating crystal up to harmonic terms is stated in Equation 10. From the corresponding energy levels in Equation 17, one can calculate the partition function of

the vibrating crystal:

$$Z = \sum_{n_{k,j}} exp(-\beta E_{nk,j}) = \prod_{k,j} \frac{exp(-\frac{\beta h w_j(k)}{2})}{1 - exp(-\beta h w_j(k))} \tag{77}$$

where $\beta = \frac{1}{k_B T}$ The internal energy follows immediately as the logarithmic derivative of the partition function.

$$E = \frac{-\partial lnZ}{\partial \beta} \tag{78}$$

The heat capacity at constant volume is the derivative with respect to temperature of the internal energy:

$$C_v = (\frac{\partial E}{\partial T})_V = k_B \sum_{k,j} \frac{(\frac{h w_i(k)}{2k_B T})^2}{sinh(\frac{h w_j(k)}{2k_B T})} \tag{79}$$

The sum is carried over different wave vectors k and different polarizations j. For a given phonon mode, the only term of the summation that depends on k is the frequency of the phonons. Finding the frequency spectrum can be approximated by Ortavy method which assumes an isotropic elastic parallelepiped of dimensions $l1, l2 \quad and \quad l3$. The equations of motion of the solid in terms of the displacement vector $U(u,v,w)$ of an atom in the solid are expressed in terms of ρ the density of the solid and (λ, μ) the Lame constants:

$$\rho \frac{\partial^2 U}{\partial t^2} = \mu \nabla^2 + (\lambda + \mu) \nabla (\nabla . U) \tag{80}$$

The boundary conditions involved express the physical realizable situation that shear stresses are zero on the boundary and that the motion perpendicular to the

boundary is zero. Solving the differential equation for the elements of U, we get:

$$\begin{aligned} u &= Asin(\frac{n_1}{l_1})cos(\frac{n_2\pi y}{l_2})cos(\frac{n_3\pi z}{l_3})exp[-iwt] \\ v &= Bcos(\frac{n_1}{l_1})sin(\frac{n_2\pi y}{l_2})cos(\frac{n_3\pi z}{l_3})exp[-iwt] \\ w &= Acos(\frac{n_1\pi x}{l_1})cos(\frac{n_2\pi y}{l_2})sin(\frac{n_3\pi z}{l_3})exp[-iwt] \end{aligned} \tag{81}$$

In order to find the frequency, we substitute the solution into Equation 80 we obtain:

$$\begin{aligned} w_l^2 &= c_l^2\pi^2(\frac{n_1^2}{l_1^2}+\frac{n_2^2}{l_2^2}+\frac{n_3^2}{l_3^2}) \\ \omega_{t_1}^2 &= c_{t_1}^2\pi^2(\frac{n_1^2}{l_1^2}+\frac{n_2^2}{l_2^2}+\frac{n_3^2}{l_3^2}) \\ \omega_{t_2}^2 &= c_{t_2}^2\pi^2(\frac{n_1^2}{l_1^2}+\frac{n_2^2}{l_2^2}+\frac{n_3^2}{l_3^2}) \end{aligned} \tag{82}$$

where

$$c_l = (\frac{2\mu+\lambda}{\rho})^{\frac{1}{2}} \quad and \quad c_t = (\frac{\mu}{\rho})^{\frac{1}{2}} \tag{83}$$

n_1, n_2 and n_3 are positive integers. However, the integers n can not run to infinity, their limiting value is set by the maximum number of atoms, i.e. the number of modes, of the crystal into consideration. At this point, all the components of Equation 114 are found, so the theoretical calculation of the heat capacity at a given temperature is made possible.

Another approach for finding the heat capacity is also provided by statistical mechanics. Starting with the same approximation of phonons by quantum oscillators, the thermal equilibrium average occupation number of phonons of wave vector **k** and polarization **j** is given by Plank distribution:

$$< n_{q,s} >= \frac{1}{exp(\frac{\hbar\omega_s(q)}{k_BT})-1} \tag{84}$$

The energy of a collection of oscillators of frequencies $\omega_j(k)$ using Plank distribution is obtained from:

$$U = \sum_q \sum_s \frac{\hbar\omega_q(s)}{exp(\frac{\hbar\omega_q(s)}{k_B T}) - 1} \tag{85}$$

The summation over q can be replaced by an integral using the density of states:

$$U = \sum_s \int D_s(\omega_q(s)) \frac{\hbar\omega_q(s)}{exp(\frac{\hbar\omega_q(s)}{k_B T}) - 1} \mathrm{d}\omega \tag{86}$$

Differentiating the internal energy with respect to temperature, we get the heat capacity:

$$C_v = \frac{\partial U}{\partial T} = k_B \sum_s \int D_s(\omega_q(s)) \frac{(\frac{\hbar\omega_q(s)}{k_B T})^2 exp(\frac{\hbar\omega_q(s)}{k_B T})}{(exp(\frac{\hbar\omega_s(q)}{k_B T}) - 1)^2} \mathrm{d}\omega \tag{87}$$

The central problem here is to calculate the phonon density of states, i.e. $D_s(\omega_q(s))$. To start with, we consider calculating the density of states in the one dimensional case and then the model can be extended to include three dimensions. A one dimensional line of length **L** carrying **N** atoms at separation **a** is restricted to vibrate with fixed ends boundaries. The first and the last atoms in the chain are fixed. Assuming that the vibrational normal modes of polarization j exhibit the standing wave pattern, the wave vector **q** will be restricted to take discrete values: $q = \frac{n\pi}{L}$ where **n** is a positive integer. The density of states is defined as the number of modes per unit frequency range for a given polarization. Thus:

$$D_s(\omega)\mathrm{d}\omega = \frac{L}{\pi} \frac{\mathrm{d}\omega}{\mathrm{d}\omega/\mathrm{d}k} \tag{88}$$

Generalizing the calculation to three dimensions, we obtain:

$$D(\omega) = \frac{\mathrm{d}N}{\mathrm{d}\omega} = \frac{Vk^2}{2\pi^2} \frac{\mathrm{d}k}{\mathrm{d}\omega} \tag{89}$$

Specifically, by considering the Debye approximation for the dispersion relation,

the density of states becomes:

$$D(\omega) = \frac{V\omega^2}{2\pi^2 v^3} \tag{90}$$

The presence of N primitive cells in the specimen under consideration would set a maximum cut off frequency ω_D given by:

$$\omega_D^3 = \frac{6\pi^2 v^3 N}{V} \tag{91}$$

After finding $D(\omega)$, the expression for the energy reduces to :

$$U = \int_0^{\omega_D} \left(\frac{V\omega^2}{2\pi^2 v^3}\right)\left(\frac{\hbar\omega}{e^{\frac{\hbar\omega}{k_B T}} - 1}\right) \mathrm{d}\omega \tag{92}$$

Defining the dimensionless variable $x = \frac{\hbar\omega}{k_B T}$, we obtain:

$$U = \frac{3V{k_B}^4 T^4}{2\pi^2 v^3 \hbar^3} \int_0^{x_D} \frac{x^3}{e^x - 1} \mathrm{d}x \tag{93}$$

We introduce the Debye temperature in terms of the cut off frequency ω_D by:

$$\theta_D = \frac{\hbar\omega}{k_B}\left(\frac{6\pi^2 N}{V}\right)^{\frac{1}{3}} \tag{94}$$

The heat capacity as a function of temperature can now be written as[32]:

$$C_v = \frac{3V\hbar^2}{2\pi^2 v^3 k_B T^2} \int_0^{\omega_D} \frac{\omega^4 e^{\frac{\hbar\omega}{k_B T}}}{(e^{\frac{\hbar\omega}{k_B T}} - 1)^2} \mathrm{d}\omega = 9Nk_B\left(\frac{T}{\theta_D}\right)^3 \int_0^{x_D} \frac{x^4 e^x}{(e^x - 1)^2} \mathrm{d}x \tag{95}$$

Comparing the two Equations 114 and 95 that give the heat capacity as a function of temperature, we find that the first one can be calculated easily once the number of atoms and the dimensions of the specimen are given, whereas the second one contains the variable of interest, that is, θ_D. Thus, the dependence of Debye temperature on temperature can be found once the summation over different wave vectors

k in equation (82) is calculated. The next step would be to solve the non-linear equation:

$$C_v = 9Nk_B(\frac{T}{\theta_D})^3 \int_0^{x_D} \frac{x^4 e^x}{(e^x-1)^2}\,\mathrm{d}x \tag{96}$$

for a given temperature **T**, the root in this case turns out to be the Debye temperature.

2. Temperature Dependent Gruneisen Parameter

After finding θ_D as a function of **T**, there remains another parameter which was assumed constant and is indeed a strong function of temperature especially at low **T**. The Gruneissen parameter is also taken as a temperature dependent. This parameter describes the effect of temperature variation on the dynamics of the crystal. Its mathematical presentation is[33]:

$$\gamma_s = \frac{-V}{\omega_s}\frac{\partial \omega_i}{\partial V} \tag{97}$$

Another indication that clarifies the dependence of both parameters comes from the idea of density of states. The idea of density of states comes to prove the dependence of the Debye parameter on temperature. The work starts from determining the density of states of phonons inside a volume, with the heat capacity (C_v) as a function of Debye parameter. As a result of dependence of both parameters on temperature, the range for calculating the thermal conductivity is widened. Therefore, this modification enhances the model and makes it more reliable.

CHAPTER III

MODELLING THE THERMAL CONDUCTIVITY IN SUPERLATTICES

Great interest in research on thermal conductivity of crystals in low dimensions has arised due to the development of experiments which allowed growth of crystals at nano-scales as well as experiments facilitating measurements in low dimensions such as Raman scattering, infrared absorption and electron diffraction at low-energy. At nano-scale, classical and quantum size effects exist because the mean free path of phonons becomes comparable to the size of the material. Heat conduction deviates significantly from classical bulk prediction values. Thermal conductivity becomes size dependent. Also by quantum predictions, size can influence conduction by affecting waves, and forming standing waves instead under the condition $n\lambda/2 = D$ [7].

Phonons obey Bose-Einstein distributions while molecules obey Boltzmann distribution, except at absolute temperature where we should consider Bose- Einstein distribution again. In nanoscale energy becomes discontinuous, and is found by SchrÃűdinger equation of phonons derived in chapter one. and since dimensions are low, then thermal conductivity can no longer be taken to be independent of position as in the case of bulks. The Boltzmann equation will hence contain an additional term contributing to a finite size in which we will have a spatial dependent distribution function.

In this chapter a discussion of phonon behaviour in nanoscales, first generally, then precisely in superlattices, will be done. I will then make an approach to calculate thermal conductivity in these systems using the obtained dispersion curves as well as my interpolation model describing phonons at interfaces.

A. Phonons in Superlattices

Superlattices are defined to be periodic layers of two types of crystals having small thickness (less than 50nm). They are grown using molecular beam epitaxy and metal-organic chemical vapour deposition which grow Superlattices of any desired thickness [34]. A major cause of the dramatic drop in thermal conductivity in superlattices compared to their bulk constituents was basically attributed to the presence of the numerous interfaces that phonons face during their propagation across the repeated layers of the superlattice. The interfaces between the layers formed a boundary that resisted propagating phonons and even scattered them due to the mismatch between the two different layers at this interface. This resulted in the limited heat dissipation in superlattices. The study of Superlattices is done by the study based on the elasticity theory. In the continuum theory, the phonons are considered to be propagating through the lattice and across boundary conditions from which we can obtain the dispersion relations.

The study of thermal conductivity across superlattices has gained great interest recently in hopes of achieving an efficient thermal management for microelectronic devices [35] [22]. Therefore, several models for describing thermal conductivity in superlattices have been demonstrated, and experimental measurements were done for the study of heat transport to obtain numerical data for different systems.

The initial treatment of superlattices as systems in which heat propagates in the form of phonons which transfer incoherently across the alternating layers have demonstrated poor resemblance to experimental expectations as will be shown in the following section of incoherent modelling of phonons in superlattices. On the contrary, some observations have found possibilities for a coherent heat transport through the lattice as if it were a bulk with no interfaces, this resulted from high wavelengths of some phonons in which periods became too small to be observed by the propagating phonon.

Our study of heat transfer starts with solving Boltzmann's equation for obtaining the phonons distribution function throughout the lattice at different temperatures and positions. Two models were suggested, where the first considers particle-like behaviour of phonons which can scatter during propagation and the second considers plane wave-like propagation in which waves transmit or reflect instead of scattering. The first model has shown a fail due to the monotonous decrease with period thickness of the superlattice, while the second approach failed at all periods above a few tens of angstroms and overestimated the expected thermal conductivity trend. An interpolation model is suggested by Latour et al.[36] where a phonon coherence length was defined as a spatial correlation of the change of atomic displacement at equilibrium due to existing phonons at a given frequency. The resulting $I_c(w)$ predicted coherent transport of phonons when the superlattice period was smaller than this correlation factor. Hence phonons will propagate in a homogeneous material with a folded Brillouin zone. And when $I_c(w)$ becomes smaller than the period, the criterion of transfer is expected to be incoherent. Though this model shows good theory, it hasn't been validated by experiments.

Our study presents an original approach for a theoretical model that demonstrates the heat transfer mechanism across superlattices by presenting an intermediate behaviour for phonons in between the coherent and incoherent propagation expected for phonons in superlattices. The coherent transport suggests that phonons transport through the superlattice assuming the material is a bulk with a folded Brillouin zone. On the other hand, the incoherent model suggests that phonons transport through the two different layers of a superlattice as if the superlattice is formed of two bulks separated by an interface. This type of interpolation was already suggested in molecular dynamics study of phonons [2]. Our interpolation is based on the multiplication of a probability factor for each type of transport. The probability is derived from considering that the phonon wavelength affects its behaviour

at the interface, a phonon with low wavelength comparable to the lattice period would undergo interface scattering whereas a phonon of high wavelength will not feel the interface as it propagates. So in general the derived model will depend on a probability that is dependent on the phonon wavelengths, the lattice period, and the root mean square irregularity of the interface in the considered superlattice. The developed model will present its results with comparison to the experimental expectations.

B. Thermal Conductivity Calculation

A major cause of the dramatic drop in thermal conductivity in superlattices compared to their bulk constituents was basically attributed to the presence of the numerous interfaces that phonons face during their propagation across the repeated layers of the superlattice. The interfaces between the layers formed a boundary that resisted propagating phonons and even scattered them due to the mismatch between the two different layers at this interface. This resulted in the limited heat dissipation in superlattices. Understanding the phonon behaviour causing this change in heat transfer will lead to modelling the thermal conductivity in these structures. Initially it was expected that the modelling of the layers as bulks separated by interfaces that are studied and included in the bulk model would give the expected results in thermal conductivity values. However, the pattern of propagation of phonons across crystals might present two modes, an incoherent transport mode, where as expected phonons scatter at interfaces and the classical study would describe heat propagation in this case, and a coherent transport mode, where phonons do not observe the interfaces but propagate through the superlattice as if it were a bulk with a folded Brillouin zone.

In the following sections we will describe both suggested models and show that phonons might propagate in either way depending on a minimal and a maximal

wavelength of the phonons.

C. The Incoherent Mode of Transport

In the incoherent propagation, phonons transmit through the first layer, then through the interface and into the second layer. The main difference between superlattices and bulks in this case is now only in accounting for the interface between each two layers. The study of phonons behaviour at the interface will be the subject of the next section.

1. Interface Thermal Conductance

Thermal conductivity was defined earlier to be the ratio of the heat current with respect to the temperature gradient [37]. The heat current is found by:

$$Q_{1\to 2} = \frac{1}{2}\sum_j \sum_q hw(j,q)n(w,T)|\mathbf{v}(j,q)\mathbf{N}|\alpha_{1\to 2}(w,i,j) \tag{98}$$

Where we have summed over all phonons incident per unit area and time. $\hbar w(j,q)$ is the phonon energy and $n(w,T) = \frac{1}{e^{\hbar w/k_B T}-1}$ is the Bose-Einstein occupation factor and $\alpha_{1\to 2}$ is the transmission probability of the phonon of frequency w to transmit from the first material to the second. The summation is done over all polarization directions j and phonon wavevectors q. $\mathbf{v}(j,k)$ is the speed of phonons of polarisation j and wavevector k. $\mathbf{N}$ is the normal to the interface directed from the first material to the second. Now, we will write the summation as:

$$\sum_K = \frac{\Omega}{(2\pi)^3}\int_0^{q_D} 4\pi k^2 dk \tag{99}$$

Where q_D is the Debye wavevector. We have that the number of modes in a sphere of radius k in the Fourier space is

$$\nu = \frac{\Omega}{(2\pi)^3}(\frac{4}{3}\pi k^3) \tag{100}$$

and we know that the density of states is given by

$$D(w) = \frac{d\nu}{dw} = \frac{d\nu dk}{dkdw} \tag{101}$$

which becomes

$$D(w)dw = \frac{\Omega}{(2\pi)^3}4\pi k^2 \tag{102}$$

Finding the heat current we can now write the thermal conductivity as:

$$\begin{aligned} TC = \frac{1}{2}\sum_j\sum_i\int_0^{w_{D,j,i}} \frac{1}{k_B T^2}(hw)^2.|v(w,i,j).N| \\ .\frac{exp(\frac{hw}{k_B T})}{[exp(\frac{hw}{k_B T})-1]^2}\alpha_{1\to 2}(w,i,j)D_{i,j}(w)dw \end{aligned} \tag{103}$$

Where j denotes one phonon polarization and i denotes a given orientation of the crystal. When the density of states and the phonon velocity is known, we need to compute the transmission probability to be able to obtain the interface boundary conductance as a function of T.

In order to get this probability at interface, two extreme models were proposed to describe the phonon modes. The first is the acoustic mismatch model (AMM), and the second is the diffuse mismatch model (DMM). The first model assumes that phonons observe the interface as a continuum surface of incidence, on which they either reflect or refract. This model works in the Brillouin zone center where we have long wavelength phonons [22]. The second corresponds to short wavelength phonons which observe the interface as a rough surface which scatters incident

phonons diffusively and phonons lose memory of their previous acoustic properties. [22] the DMM assumption hence predicts non-conservative momentum. Thus, both models present limitations on their predictions. An intermediate solution is thus necessary to describe phonons behaviour at interface. Kazan, M. et al. [22, ..] have suggested a complete model of interpolation between DMM and AMM in which they showed calculations depending on the characteristics of phonons and surfaces. Also, this model presented a more accurate study by considering the detailed phonon dispersion relations instead of the limited linear Debye approximations considered in the previous models. This has improved thermal conductivity resemblance to experimental measurements. In the following section we provide a thorough description of phonons at interfaces, first as derived by each of the extreme models, then the interpolating model will be discussed.

a. The Acoustic Mismatch Model

In the acoustic mismatch model, phonons are treated as waves propagating in a continuous medium. This is valid when their wavelengths are much larger than the interface asperities. Hence, when a phonon reaches an interface between two crystalline materials, the case would be a case of a wave incident on an interface of two mediums. Therefore, it is expected of this wave to either reflect or refract into the second material. Reflection can be specular or with polarization conversion. Refraction may convert polarization too. Thus the phonon here will be governed by Snell's law. Starting with the case of no polarization conversion, if θ_1 is the angle between the wavevector and the normal to the interface, then the wave will refract into the second medium such that it satisfies the following law:

$$sin\theta_2 = \frac{v_2(w,i,j)}{v_1(w,i,j)} sin\theta_1 \tag{104}$$

where $v_2(w,i,j)$ is the wave speed in the second material. The interface is assumed to be a perfectly smooth surface. Now, if the incident wave has an angle larger than the critical angle, the wave will undergo reflection. The transmission critical angle is found by the formula:

$$\theta_{1,max} = v_1(w,i,j)/v_2(w,i,j) \tag{105}$$

Phonons having an angle less than this limiting angle will transmit with a transmission probability of:

$$\alpha_{1\to 2(AMM)}(w,i,j) = \frac{4Z_1Z_2\mu_1\mu_2}{(Z_1\mu_1+Z_2\mu_2)^2} \tag{106}$$

Where $\mu = cos\theta$ and Z is the acoustic impedance which is the phonon speed multiplied by the density of the material: $Z = \rho v(w,i,j)$. For phonon incident at an angle larger than the limiting angle, the probability of transmission or refraction will be zero. The probability of reflection can then be written as:

$$R_{1\to 2(AMM)}(w,i,j) = 1-\alpha_{1\to 2(AMM)} = |\frac{Z_1\mu_1 - Z_2\mu_2}{Z_1\mu_1+Z_2\mu_2}| \tag{107}$$

Assuming the AMM, the interface is treated as a perfectly smooth plane. This assumption is thus valid only when the wavelengths of the phonon plane waves are much greater than the interface asperities.

b. The Diffuse Mismatch Model

In the DMM, the acoustic correlations at the interface are assumed to be completely destroyed by elastic diffuse scattering, so that the only determinants of the transmission probability are the phonon densities of states of the materials in contact [38]. The probability of transmission is nonetheless determined by a mismatch between

densities of state. The transmission probability from side 1 to side 2 of the interface can be written in the DMM as

$$\alpha_{1\to 2(DMM)}(w,i,j) = \frac{\sum_{i,j} \nu_2(w,i,j).D_2(w,i,j)}{\sum_{i,j} \nu_2(w,i,j).D_2(w,i,j) + \sum_{i,j} \nu_1(w,i,j) + D_1(w,i,j)} \tag{108}$$

This equation is derived from the principle of detailed balance [38]. The maximum transmission probability for a phonon from side 1 to side 2 when the phonon densities of states at both sides of the interface match with each other. However, if an interface is considered between two solids with identical acoustic phonon properties, the transmission probability according to AMM is unity, whereas the transmission probability in the DMM is exactly 0.5. We can deduce then that the DMM gives a prediction of a finite thermal resistance at an imaginary interface in the material.

c. The Interpolation Model

The phonon transmission coefficients appeared to come very close to those predicted by the AMM, at least for phonons with large wavelengths, or alternatively, low frequencies (less than 300 GHz). In the particular case of solid/solid interface, the thermal conductance of the interface was actually lower than that predicted by the AMM. The most thoroughly studied interfaces were those between sapphire and indium [39][40]. In these experiments, the measured interface thermal conductance for different samples varied significantly, depending on the details of the sample preparation. The temperature dependence was also not as expected from the AMM. However, measurements of the thermal conductance between sapphire and Aluminium showed a close agreement with the AMM [39]. The occasional disagreement with the AMM was attributed to an imperfect physical contact between the materials. In both AMM and DMM the thermal conductance contained large contributions from the phonon scattering, and transmission at the interfaces could

not be deduced accurately. This suggests that the interface thermal conductance can be described accurately by the AMM only at low enough temperatures. It was found from phonon reflectivity experiments that phonons in the frequency range above a few hundred GHz are strongly scattered at all but the most carefully prepared surfaces. All these experimental observations suggest that at low temperatures, when the incident phonons are of wavelengths larger than the interface asperities, the phonon scattering at the interface is unlikely and the AMM fails to describe the interface thermal conductance. However, at high temperatures where phonons from the Brillouin zone carry the heat, the DMM is more appropriate than the AMM to describe the interface thermal conductivity. Nevertheless, at intermediate temperatures, where both specular and diffuse transmission are expected, neither the AMM nor the DMM can describe accurately the interface thermal conductance. Thus, a model that takes into account the interface conditions and interpolates between the AMM and the DMM is certainly needed to describe quantitatively the interface thermal conductance in the full temperature range. Likely, neither the AMM nor the DMM can describe accurately the interface thermal conductance. Thus, a model that takes into account the interface conditions and interpolates between the AMM and the DMM is certainly needed to describe quantitatively the interface thermal conductance in the full temperature range. Phonon dispersion relationship is usually approximated by a linear relationship (the Debye approximation). However, the Debye approximation is justified only for wavevectors close to the Brillouin zone center, because away from the BZ center there is a significant deviation between the real phonon dispersion relationship and the phonon dispersion obtained from the Debye approximation. Therefore, below the Debye temperature, where only phonons of small wavevectors carry the heat, the Debye approximation is reasonable. In fact, it has been demonstrated that the Debye approximation causes a large error in the calculation of the interface TC [41].

According to a statistical model by Ziman a plane wave incident on a rough surface

reflects as a plane wave in the direction of specular reflection and a contribution with a finite angular spread about that direction. The result is an average flux density in a given direction with the formula:

$$\begin{aligned} < |F(\alpha,\beta,\gamma)|^2 >_{AV} = exp(-\gamma^2 < \phi^2 >)\delta(\alpha)\delta(\beta) \\ +B[\frac{L^2}{4\pi}exp(-\gamma^2 < \phi^2 >) \sum_{n=1}^{\infty} \frac{(\gamma^2 < \phi^2 >)^n}{n!n} \\ .exp[-(\frac{L^2}{4n}(\alpha^2+\beta^2)] \end{aligned} \tag{109}$$

where,

$$\begin{aligned} \phi(x,y) &= \frac{2\pi}{\lambda} z(x,y) \\ \alpha(\Omega_0,\Omega) &= (\frac{2\pi}{\lambda}).(sin\theta_0 cos\phi_0 - sin\theta cos\phi) \\ \beta(\Omega_0,\Omega) &= (\frac{2\pi}{\lambda}).(sin\theta_0 sin\phi_0 - cos\theta cos\phi) \\ \gamma(\theta_0,\theta) &= cos\theta_0 + cos\theta \end{aligned} \tag{110}$$

with $\Omega_0 = (\theta_0, \phi_0)$ and $\Omega = (\theta, \phi)$ referring to the directions of the incident and emerging wavevectors, respectively, and $\phi(x,y)$ being the one way phase shift caused by deviation from the plane z=0. In addition to an average roughness, the surface is described here by a tangential correlation length (L). The proportionality constant B, determined from the flux conservation condition, is found to be

$$B(\Omega_0) = \frac{\varepsilon(\Omega_0)[1 - p_s(\theta_0)]}{c(\Omega_0)} \tag{111}$$

with

$$\begin{aligned} \varepsilon(\Omega_0) &= \int d\Omega \delta(\alpha) \\ \delta(\beta) &= (\frac{\lambda}{2\pi})^2 sec(\theta_0) \\ p_s(\theta_0) &= exp(-4 < \phi^2 > cos^2\theta_0) \\ c(\Omega_0) &= \int d\Omega_c(\Omega_0,\Omega) \end{aligned} \tag{112}$$

The average flux density in its actual form can be seen as the sum of a specular part

$p(\theta_0,\theta)$ and the diffusive $c(\Omega_0,\Omega)$. Thus, for simplicity one can write the equation of the average flux density as:

$$< |F(\alpha,\beta,\gamma)|^2 >_{AV} = \left[p(\theta_0,\theta).\delta(\beta) + B(\Omega).c(\Omega_0,\Omega) \right] \tag{113}$$

2. Calculating the Probability of Transition at Interfaces

Let $P(\Omega_0,\Omega)$ now be the transition probability of the phonon plane wave per unit solid angle from Ω_0 to Ω. With

$$P = \int P(\Omega_0,\Omega) d\Omega_0 \tag{114}$$

and since $P(\Omega_0,\Omega)$ is by definition the average flux density normalized to unity, then it can be expressed by:

$$P(\Omega_0,\Omega) = [\frac{1}{\varepsilon(\Omega_0)}] p(\theta_0,\theta)\delta(\alpha)\delta(\beta) + \varepsilon(\Omega_0)[\frac{1-p_s(\theta_0)}{c(\Omega_0)}] c(\Omega_0,\Omega) \tag{115}$$

We insert this expression of $P(\Omega_0,\Omega)$ in the integral, equation 114, to get the following expression for P at the z = 0 surface

$$p = \int P(\Omega_0,\Omega) d\Omega = p_s(\theta_0) + \int [1-p_s(\theta_0)][\frac{c(\Omega_0,\Omega)}{c(w_0)}] d\Omega_0 \tag{116}$$

Take $\Delta(\Omega_0,\Omega) = \int \left[1-p_s(\theta_0)\right] \left[\frac{c(\Omega_0,\Omega)}{c(w_0)}\right] d\Omega_0$ then equation 116 can be written as

$$P = p_s(\theta_0) + \Delta(\Omega_0,\Omega) \tag{117}$$

The probability for a specular reflectivity is determined by $p_s(\theta_0)$ whereas the probability for diffuse reflectivity is given by $\Delta(\Omega_0,\Omega)$. From equation 116, we can recover the limiting cases: when L goes to zero, the term $\Delta(\Omega_0,\Omega)$ becomes neg-

ligible and thus specular reflectivity is the dominant mechanism. However, for a completely correlated interface,

$$c(\Omega_0, \Omega) \rightarrow [1 - p(\theta_0, \theta)]\delta(\alpha)\delta(\beta) \tag{118}$$

which yields $B(\Omega_0) = 1$ and $\Delta(\Omega_0, \Omega) = 1 - p_s(\theta_0)$. Physically, that is the situation when locally the surface becomes practically a plane resulting in the merge of diffuse part of the emerging flux with the specular part. From Equation 117, we can express the directional dependence of the probability of reflection at the interface as the weighted average of the reflection probability derived from acoustic mismatch model and diffuse mismatch model.

$$r_t = p_s(\theta_0)R_{sp} + \Delta(\Omega_0, \Omega)R_d \tag{119}$$

R_{sp} represents the specular reflectivity and R_d the diffuse reflectivity. Finally, we reach an expression giving the transition probability which is the quantity of interest in the calculation of thermal conductance at the interface between two solids:

$$\alpha_{1\rightarrow 2}(w, i, j) = 1 - r_t(w, i, j) \tag{120}$$

At this level, calculation of thermal conductance becomes a matter of computing transmission probability between the two interfaces as described above and then replacing its expression in the main integral expression of thermal conductance.

3. Incoherent Thermal Conductivity Calculation

For the case of superlattices, phonons were expected to propagate incoherently through the crystal, due to the repeated interface. The thermal conductivity is considered to be a weighted average of the thermal conductivity in each layer including

the effect of boundary resistance. If d_1 and d_2 are the thicknesses and κ_1 and κ_2 are the thermal conductivities of the first and second layer respectively,

$$\kappa_{inc} = \frac{d_{SL}}{(\frac{d_1}{\kappa_1} + \frac{d_2}{\kappa_2}) + 2R_B} \tag{121}$$

where $d_{SL} = d_1 + d_2$ and $R_B = \frac{R_B(1\to2)+R_B(2\to1)}{2}$ $R_B(1 \to 2)$ is the interface thermal resistance of phonons at the interface [42]. The boundary scattering at the interface between the layers will have a relaxation time given by [41]:

$$R_B(x \to y) = \left[\frac{1}{2}\sum_{[hkl]}\sum_{j}\sum_{q}\frac{1}{k_B T^2}\hbar^2 w_j^2(q_{hkl})v_j(q_{hkl})\frac{exp(\frac{\hbar w_j(q_{hkl})}{k_B T}}{\left[exp(\frac{\hbar w_j(q_{hkl})}{k_B T} - 1\right]^2}\sigma_j(q_{hkl})\right]^{-1} \tag{122}$$

$\sigma_j(q_{hkl})$ is the transmission probability of the phonons of polarization j and wavevectors q_{hkl}. This transmission probability is calculated from an interpolation between two models: the acoustic mismatch model and the diffuse mismatch model [43]. Having calculated all the needed variables, the values for the thermal conductivity at different temperatures can be obtained.

In figure 6, it can be seen that plotting the obtained results of calculation provide a logical trend but do not fit the experimental measurements. The modelling of phonon propagation by a purely incoherent model is hence not accurate.

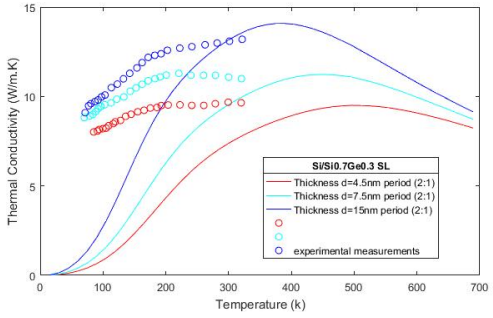

Figure 6: Thermal conductivity of $Si/Si_{0.7}Ge_{0.3}$ superlattices as predicted by the study of the incoherent transport of phonons

D. The Coherent Mode of Transport

Although the assumptions given for the incoherent modelling are realistic for superlattices, the resulting calculations give poor fitting with the real values of thermal conductivity in superlattices. This means that the incoherent propagation is not in complete control of phonons propagation. In this section, we will adapt the previous results of the Boltzmann equation for modelling a coherent phonon transport in superlattices.

1. Continuum Model of Phonons in Superlattices

When the acoustic phonons in a crystal have a wavelength greater than the lattice atomic scales, the atomic displacement is taken to be a continuous displacement. And thus phonons will be treated as elastic waves. These waves will be propagating in the crystal anisotropic media. We consider two media, which will constitute the layers of the superlattice. They are characterized by densities $_1$ and $_2$, and elastic constants Ω_1 and Ω_2, and the waves are taken to be propagating in the z-direction chosen to be also the direction of the growth of the superlattice. To study the wave propagation in this case, we start with the general equation of motion:

$$\rho_{1,2}\frac{\partial^2 u}{\partial t^2} = \frac{\partial \sigma_{1,2}}{\partial z} \tag{123}$$

where $\sigma_{1,2}$ represents the stress tensor of the form:

$$\sigma_{1,2} = \Lambda_{1,2}\frac{\partial u_{1,2}}{\partial z} \tag{124}$$

then the equation of motion becomes:

$$\rho\frac{\partial^2 u}{\partial t^2} = \frac{\partial}{\partial z}(\Lambda\frac{\partial u}{\partial z}) \tag{125}$$

For a monochromatic elastic wave, one can seek a solution from the boundary conditions:

1. Stress is continuous at interfaces:

$$\Lambda_1 \frac{\partial u_1}{\partial z} = \Lambda_2 \frac{\partial u_2}{\partial z} \tag{126}$$

2. Displacement is continuous at interfaces,

$$u_1 = u_2 \tag{127}$$

3. Displacement is represented by a Bloch wave:

$$u(z+d) = u(z)e^{iqd} \tag{128}$$

Where the periodicity is given by $d = d_1 + d_2$; with d_1 and d_2 the periodicities in the first and second materials respectively. The relation between w and q is obtained from applying the above conditions on the equation of motion:

$$(\rho_{1,2} w^2 - \Lambda_{1,2} q^2) u_{1,2} = 0 \tag{129}$$

Which is a cubic equation in frequency. The roots of this equation give the frequency as a function of the wavevector q:

$$w = \sqrt{\frac{\Lambda_{1,2}}{\rho_{1,2}}} q_{1,2} \tag{130}$$

Where $q_{1,2}$ are the wavevectors in the superlattice, found from the relation with the wavevectors of bulks:

$$\frac{q}{q_{1,2}} = \frac{d_{1,2}}{d} \tag{131}$$

To solve the equation of motion, we use the trial solutions:

$$u_1(z) = (Ae^{iq_1 z} + Be^{iq_1 z})e^{-iwt} \tag{132}$$

And

$$u_2(z) = (Ce^{iq_2 z} + De^{-iq_2 z}e^{iwt}) \tag{133}$$

Substituting these solutions into the boundary conditions we get the following conditions on A, B, C and D: At z=0:

$$A + B = C + D \tag{134}$$

which gives:

$$(A - B)\Lambda_1 q_1 = (C - D)\Lambda_2 q_2 \tag{135}$$

and at $z = d_2$:

$$Ce^{iq_2 d_2} + De^{-iq_2 d_2} = (Ae^{-iq_1 d_1} + Be^{iq_1 d_1}e^{iqd}) \tag{136}$$

which gives:

$$\Lambda_2 q_2 (Ce^{iq_2 d_2} - De^{iq_2 d_2}) = \Lambda_1 q_1 (Ae^{-iq_1 d_1} - Be^{iq_1 d_1})e^{iqd} \tag{137}$$

For $-d_1 \leq z \leq 0$:

$$u_1 = (\Lambda_1 q_1 sin(q_2 d_2))cos(q_1 z) - (\Lambda_2 q_2 cos(q_2 d_2))sin(q_1 z) + (\Lambda_2 q_2 e^{iqd})sin(q_1(q_1(z+d_1)) \tag{138}$$

and for $0 \leq z \leq d_2$

$$u_2 = (\Lambda_1 q_1 e^{iqd} cos(q_1 d_1))sin(q_2 z) + (\Lambda_2 q_2 e^{iqd})sin(q_1 d_1))cos(q_2 z) - \Lambda_1 d_1 sin(q_2(z - d_2)) \tag{139}$$

And we also obtain the dispersion curve for phonons:

$$cos(qd) = cos(q_1 d_1)cos(q_2 d_2) - \frac{\Lambda_1\rho_1 + \Lambda_2\rho_2}{2\sqrt{\Lambda_1\rho_1\Lambda_2\rho_2}} sin(q_1 d_1)sin(q_2 d_2) \tag{140}$$

The obtained equation can be also written in the form:

$$cos(qd) = cos(w(\frac{d_1}{v_1} + \frac{d_2}{v_2})) - \frac{\varepsilon^2}{2} sin(\frac{wd_1}{v_1})sin(\frac{wd_2}{v_2}) \tag{141}$$

Where ε is a constant that measures the mismatch of the acoustic impedance of the two lattices corresponding to each of the materials 1 and 2 and it has the value of:

$$\varepsilon = \frac{\Lambda_1\rho_1 - \Lambda_2\rho_2}{\Lambda_1\rho_1 + \Lambda_2\rho_2} \tag{142}$$

Taking the special case of long wavelengths, where q and w approach zero, the dispersion relation takes again the linear Debye form w=qv, where

$$v = d[(\frac{d_1}{v_1} + \frac{d_2}{v_2})^2 - \varepsilon^2(\frac{d_2}{v_2})(\frac{d_1}{v_1})]^{-\frac{1}{2}} \tag{143}$$

When ε is small, the second term in the general dispersion curve splits the frequency values, at the center and edges of the Brillouin zone. So we get at the center new optical modes which have an acoustic nature. A representation of the folded acoustic curve of the superlattice is shown in Figure 7 obtained from the above continuum theory. As can be seen, the dispersion curve represents small splitting at the zone center and edges. In the figure, a dashed curve is represented to show the curve of a bulk of similar materials and of thickness $\bar{d}_{(1,2)}$. Ian 1979, Narayanamurti et al. observed the folding of the Brillouin zone and the creation of minigaps and verified them experimentally by acoustic transmission of superconducting tunnel junctions. Later Colvard et al. (1980) and Jusser and et al. (1987) also obtained the same results by Raman Scattering.

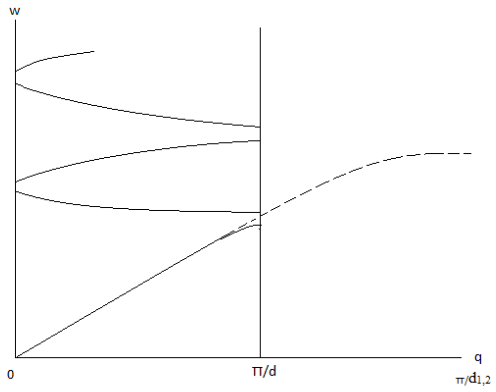

Figure 7: The folded dispersion curve of a superlattice obtained by the continuum theory. Dashed curve corresponds to a dispersion curve a similar bulk structure

The obtained plot of the dispersion relation will be used in calculating the phonons velocity in the coherent model to obtain thermal conductivity from the coherent phonon propagation.

2. Coherent Thermal Conductivity Calculations

Then this model will be interpolated with the incoherent model to obtain a corrected formula for thermal conductivity in superlattices. The coherent model assumes the superlattice as an interface-free bulk restricted by the folded Brillouin zone of superlattices. We will apply this assumption on superlattices and obtain a new formula for thermal conductivity. By plotting the obtained dispersion relation in the study of superlattices, we can calculate the group velocity of phonons from the slopes of the branches of the obtained curve. Now the calculation of thermal conductivity in the coherent model can be obtained. The resulting values of thermal conductivity are presented in figure 8. It is clear that the coherent model provides a logical match of the thermal conductivity measurements only at low periods and low temperature as in the the case of a period of 4.5 nm at temperatures below 200, and they present close values at higher temperatures in this thickness.

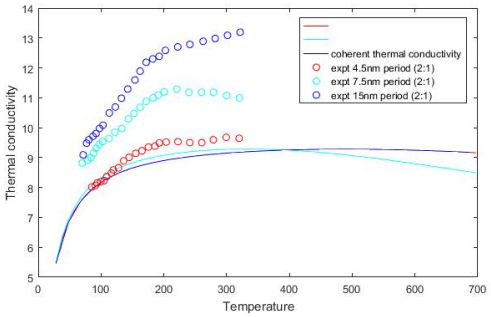

Figure 8: Thermal conductivity of $Si/Si_{0.7}Ge_{0.3}$ superlattices as predicted by the study of the coherent transport of phonons

CHAPTER IV

RESULTS

A. Modelling Thermal Conductivity With Temperature Dependent Vibrational Parameters

In chapter two we presented a general formalism for describing thermal conductivity in bulk structures with distinguishing normal and Umklapp phonon processes as well as including the effect of all high symmetry directions in the lattice. then we modified the model adapted by Callaway to include temperature dependent Debye temperature and Gruneisen parameter. The resulting formula is then plotted to show the improvement in the fitting of thermal conductivity values with the experimental measurement.

Demonstration of our model is presented in Figure 9. Thermal conductivity is calculated by our model for various bulks as well as in thin film samples. Excellent fitting is observed between the measured values and our expectations. Our model can be hence used for also predicting thermal conductivity values in low or high temperatures were measurements values aren't available yet. The code used will also be expected to give correct calculations for finding thermal conductivity predicted by the incoherent model.

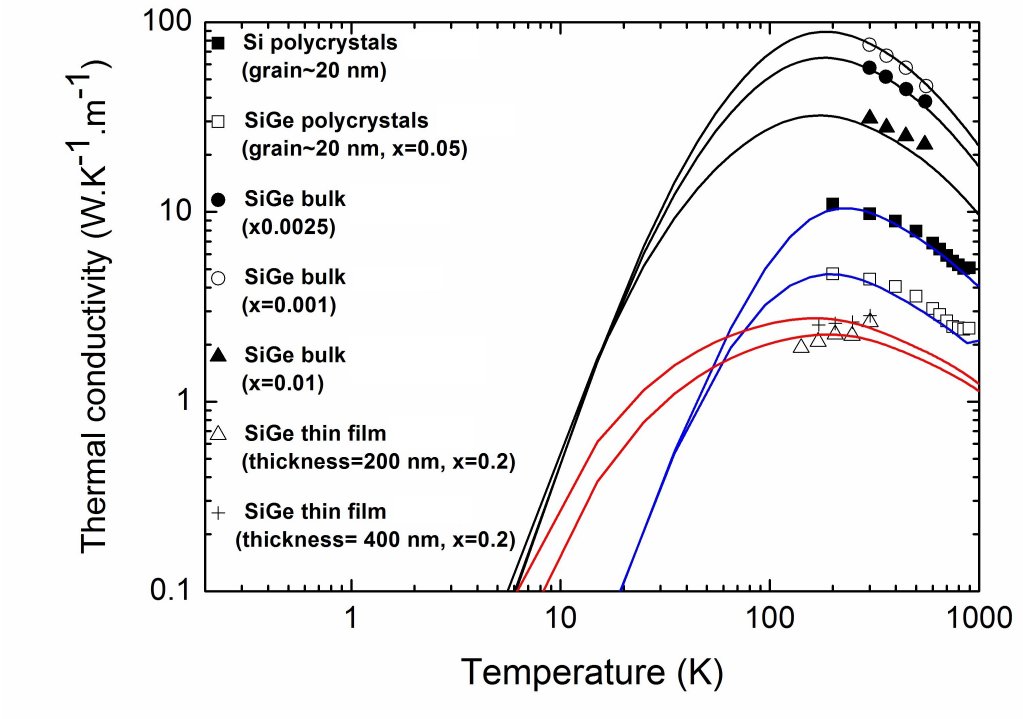

Figure 9: calculation of thermal conductivity as a function of temperature in bulks, polycrystals and thin films of different thicknesses. Experimental values are from reference [44] for polycrystals,[45] for thin films and [46] for bulks.

B. Modelling Thermal Conductivity in SiGe Superlattices

The obtained formula of thermal conductivity is applied on $Si/Si_{0.7}Ge_{0.3}$ and $Si_{0.84}Ge_{0.16}/Si_{0.76}Ge_{0.24}$ superlattices and the plots reproduced the experimental measurements. Then this paper focused on developing a predictive model that provides a tool to optimize a superlattice structure of minimal thermal conductivity. Deposition and characterization of the optimized structures represent a challenging experimental task in materials engineering due to the emergence and serious need of high efficient thermoelectric devices in various technological domains. So after demonstrating the accuracy of this model a mesh of thermal conductivities of superlattices of varying compositions is demonstrated to suggest a composition which gives a minimal thermal conductivity at 300k and 700k. The results show that su-

perlattices can be a potential material for a new generation of high-efficiency high temperature thermoelectric devices suitable for applications which require thermal insulation in nanoscales such as aerospace engineering microelectronics, optical communications, and semiconductor processing equipment. In order to show the precision of the resulting model for superlattices, the obtained thermal conductivity is evaluated for $Si/Si_{0.7}Ge_{0.3}$ and $Si_{0.84}Ge_{0.16}/Si_{0.76}Ge_{0.24}$ superlattices of different periods as a function of temperature and the resulting values were compared to the known experimental observations. As seen before, plotting the thermal conductivity obtained from the incoherent transport of phonons, Figure 6, shows poor resemblance to the reported experimental curves [40]. As the temperature and period increase, the discrepancy between experimental and incoherent modelling decreases as in the case of $Si/Si_{0.7}Ge_{0.3}$ for a thickness of 30 nm and a temperature above 200k. In this case we get a satisfactory agreement in the results. For the coherent transport, Figure 8, thickness does not make a noticeable effect on the values of thermal conductivity due to neglecting boundaries in this model.

An investigation of phonon behaviour suggests that heat transport is actually the result of a mixed transportation mode. The thermal energy k_BT that excites the phonons at energy levels smaller or equal to k_BT. So at temperature T, the excited phonons are characterized by a frequency w satisfying :

$$w = \frac{2\pi v}{\lambda} \leq k_BT \tag{144}$$

for a phonon at a specific temperature and of frequency w.

Thus, at temperature T, the shortest excited wavelength is related to T according to $\lambda_{min} \approx \frac{2\pi\hbar v}{k_BT}$ and the longest excited wavelength is given by $\lambda_{max} = \frac{2\pi}{q_{min}}$ where $-q_{min} = 2\pi/l_1$ The result is that if the superlattice period and the rms irregularity are smaller than the minimum wavelength, then the phonons will behave as if they

see all the interfaces simultaneously and hence will propagate coherently along specific paths decided by the folded dispersion curve in a perfect harmonic way. This is the case when the period and the temperature are low. The incoherent transport will dominate if on the contrary the period and the rms irregularity h exceed the maximum wavelength because the phonons will scatter due to the boundaries. Short wavelength phonons can't observe all interfaces and hence will interact with each interface separately according to the boundary resistance study. This is the case when the temperature and period increase. We can then expect the transport to be intermediate between these two cases and the weight of each mode will be determined by the temperature, period and rms irregularity h since these are the variables between each of the extreme models. Therefore, the probability of the coherent phonon heat transport increases as λ_{min} increases and the period decreases. Since λ_{min} is inversely proportional to T, the coherent phonon heat transport becomes more likely as both T and d_{SL} decrease. On the contrary the incoherent phonon heat transport becomes more favorable as both T and d_{SL} increase. Therefore, the phonon heat transport mode in a superlattice can be reasonably considered as a mixed transport mode ensured by both coherent and incoherent phonons and the contribution of each is determined by the temperature T, the rms irregularity h at the interface, and the period thickness. The obtained mixed thermal conductivity will then have the form:

$$\kappa = \kappa_{coh}\left[1 - exp\left(\frac{-\lambda_{min}^2}{d_{SL}h}\right)\right] + \kappa_{inc}\left[1 - exp\left(\frac{-d_{SL}}{\lambda_{max}}\right)\right] \tag{145}$$

The coherent model of thermal conductivity is represented by κ_{coh} , whereas the incoherent model is represented by κ_{inc}. It is obvious that for low periods κ_{coh} dominates while κ_{inc} dominates for periods much higher than the maximum wavelength. Without any loss of generality, we consider here that h is always smaller than d_{SL}. With this form of κ, it can be seen that in the limit where λ_{min} is much larger than

d_{SL} and h, κ reduces to κ_{coh}, whereas in the limit where λ_{max} is much smaller than d_{SL}, κ reduces to κ_{inc}. Using the dispersion relation and the formulas of minimum and maximum wavelengths, we can write the mixed thermal conductivity as

$$\kappa = \kappa_{coh}\left[1 - exp\left(\frac{-4\pi^2\hbar^2v^2}{k_B^2T^2d_{SL}h}\right)\right] + \kappa_{inc}\left[1 - exp(-2)\right] \tag{146}$$

The reduced form shows that the incoherent transform will always be constant in the transport while the coherent transport will depend on temperature, period, rms irregularity and the phonon group velocity. So the incoherent transport is always included in the phonon transport while the coherent transport can never dominate. Using this obtained formula, a plot of the thermal conductivity of superlattices of variable thicknesses of $Si/Si_{0.7}Ge_{0.3}$ and $Si_{0.84}Ge_{0.16}/Si_{0.76}Ge_{0.24}$ is presented in Figures 10 and 11 with a comparison to experimental values. The surface roughness is used as an adjustable parameter. The resulting plots show excellent match to the expected values, which indicates that indeed the phonon propagation is not purely incoherent but obeys the mixed model presented in this paper.

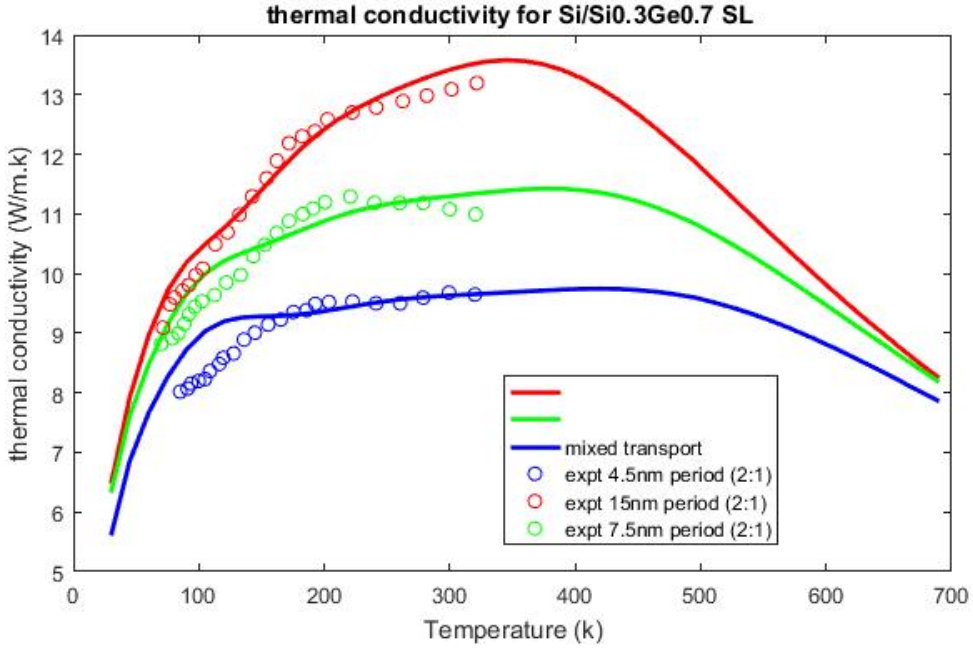

Figure 10: Thermal conductivity in $Si/Si_{0.7}Ge_{0.3}$ superlattices resulting from the mixed transport of phonons in comparison with experimental measurements

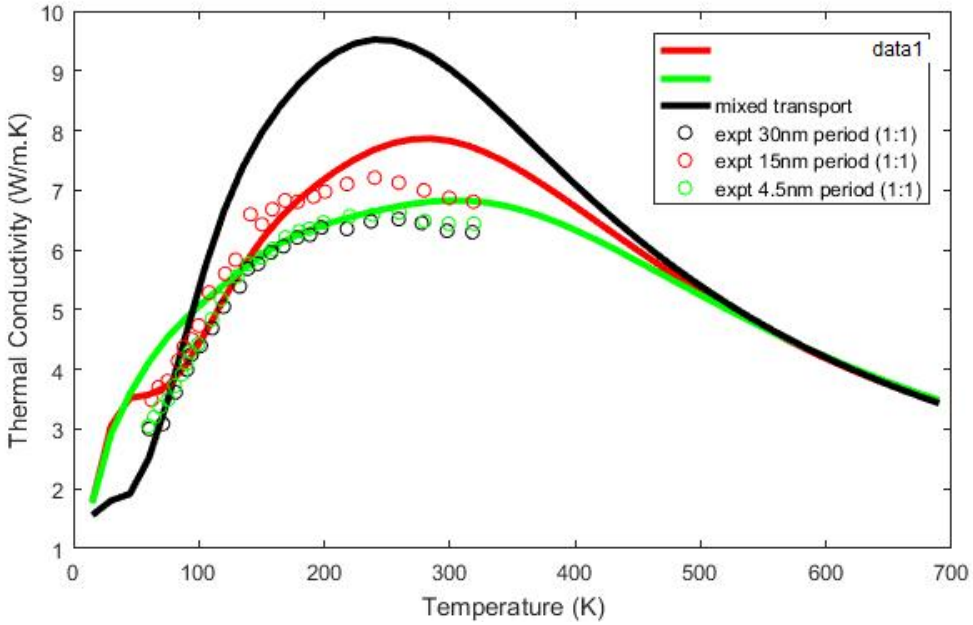

Figure 11: Thermal conductivity in $Si_{0.84}Ge_{0.16}/Si_{0.76}Ge_{0.24}$ superlattices resulting from the mixed transport of phonons in comparison with experimental measurements

C. Optimization of a Superlattice with Minimal Thermal Conductivity for Thermoelectric Applications

The requirements of low thermal conductivity for low dimensional materials have shown to be unsatisfied by the simple bulk semiconductors, and the proposed solution was the design of a superlattice of crystalline layers of different materials. These artificial materials have demonstrated a strongly reduced thermal conductivity that improved the performance of thermoelectronics as well as other applications. In this section, we will use this model to optimize a superlattice of $Si_xGe_{1-x}/Si_yGe_{1-y}$ of minimal thermal conductivity which can be a satisfactory material for thermoelectric applications. Si and Ge are always favourable elements in semiconductor industry for their excellent performance and simple acknowledgement of all of their properties. Having verified the accuracy of this model of mixed transport, we can suggest an expectation of the best period and superlattice composition that possesses a minimal thermal conductivity. A detailed calculation of ther-

mal conductivities of superlattices as a function of varying compositions is done at temperatures of 300k and 700k for different thicknesses in order to observe a minimal thermal conductivity. The resulting mesh is presented in Figure 12. the compositions of the Superlattices of $Si_xGe_{1-x}/Si_yGe_{1-y}$ are varied from x=0 to x=1 with a step of 0.1 for the first layer, where x represents the relative composition of germanium in the first layer and from y=0 to y=1 with a step of 0.1 for the second layer, where y represents the relative composition of germanium in the second layer of the $Si_xGe_{1-x}/Si_yGe_{1-y}$ superlattice. Hence the calculations are done over eleven different compositions in the first layer as well as eleven different compositions of the second layer. The result will be a calculation of thermal conductivities of 121 different superlattices. The calculations will be done at three different temperatures 300^ok, 700^ok and 1300^oK and 3 different thicknesses of 30, 15 and 7.5nm.

The meshes obtained represent the values of thermal conductivity. At the upper left and lower right corners, one can see that the case corresponds to bulks of Si (x=y=0) and Ge (x=y=1) respectively. And hence the thermal conductivity for these two compositions will be much higher than the other cases which will be the cases of superlattices. Similarly, the upper right corner and lower left correspond to Si/Ge superlattices which also demonstrate higher thermal conductivities than superlattices made of alloys due to the jump in relaxation time because of scattering by mass defect in alloys which are represented by the blue squares of the given meshes. It can be seen from the meshes that in general as the compositions get higher than 0.5, the thermal conductivities get smaller. The diagonal elements demonstrate layers of same compositions so it is expected that they should hold approximately similar heat propagation as that in bulks with the same composition since no interface will be existing, as long as the surface roughness is the same. The Lower temperature, 300k, as expected also gives higher thermal conductivity.

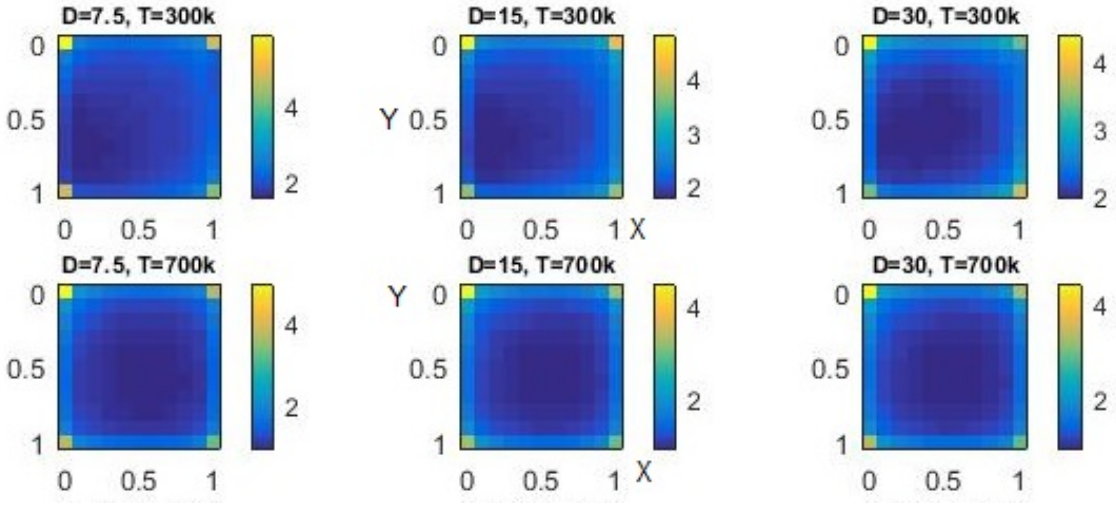

Figure 12: calculation of superlattice thermal conductivity as a function of alloy compositions for different thicknesses and temperatures

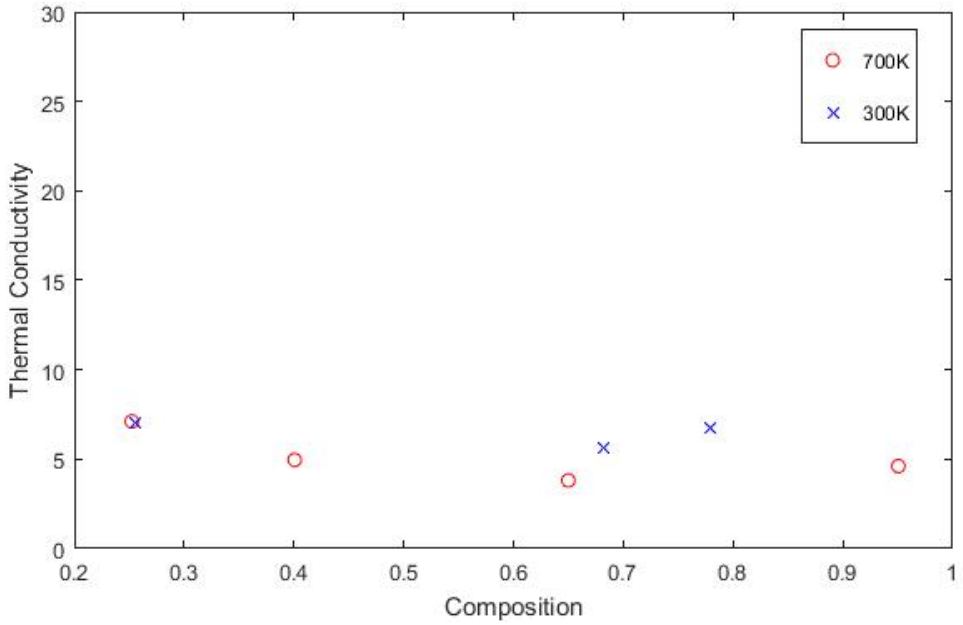

Figure 13: calculation of bulk thermal conductivity as a function of alloy compositions for different thicknesses and temperatures[47]

We first started with a mesh of $Si_xGe_{1-x}/Si_yGe_{1-y}$ as a function of x and y and for a thickness of 30nm and at temperature of 300k, the minimum is found to be at x= 0.7 and y= 0.1 with a value of 4.7. This minimum drops to 2.5 at T=700k and it occurs at x, y= 0.6. in all the cases under study, the lowest possible value of thermal

conductivity occurs at D=15 nm, with a value of 2.5 for the thermal conductivity occurring at x=y= 0.6 at T=700k. This minimum however corresponds to a bulk and not a superlattice since the compositions are identical, hence we can expect that the effect of alloys is the only reason behind the low thermal conductivity here. For T=300k the minimal thermal conductivity that can be attained is at D=7.5nm with x=0.7 and y=0.1, with TC(min)=4.7, which demonstrates the effect of the interface in lowering the thermal conductivity since for the bulk case of composition 0.1 or 0.7 the thermal conductivity ranges between 7-10 $W.k^{-1}m-1$ for T=300k. Now, in order to observe these minima and check whether superlattices and the impact of their interfaces has an effect on lowering thermal conductivity, we can compare the obtained values with the plot of thermal conductivity of bulks as a function of variable compositions, Figure 13. It can be seen from the plot that the minimal thermal conductivity for 300k is $6W.k^{-1}m^{-1}$ for a composition of 0.8, whereas in the usage of a superlattice the thermal conductivity can drop as far as 4.77 for compositions of 0.7 in the first layer and 0.1 in the second. This is expected since at high temperature the effect of compositions increases. Whence the superlattice with its interface effect has achieved a decrease by 20% in the thermal conductivity values. Consequently, 7.5nm thick $Si_{0.3}Ge_{0.7}/Si_{0.9}/Ge_{0.1}$ superlattice at 300k can be considered as a potential PGEC material for SiGe-based high-efficiency thermoelectric devices operating at high temperatures.

D. Applications

Our study provides a useful tool for many applications in nanoscale. we mention some domains of industry where a thermal conductivity model of superlattices is useful:

1. In the nanoelectronics of processors, heating problems have led manufacturers to slow down the miniaturisation trend by switching to multi-unit structures in

which several computing units are integrated into the same chip.

2. Data storage will for its part be heat-assisted. Heating can activate or inhibit magnetisation reversal. It can also change the phase or the geometry of a storage medium, and this over nanoscale areas.

3. Thermoelectric energy conversion is currently undergoing a revolution through manipulation of the thermophysical properties of nanostructured materials. In 2002, certain superlattice alloys were able to produce an intrinsic performance coefficient twice as high as had ever been measured for a bulk solid material. This breakthrough was achieved by improving thermal properties. In all these fields of application, our understanding of the relevant heat mechanisms and the associated modelling tools remains poor or at best imperfect.

CHAPTER V

SUMMARY AND FUTURE WORK

In this thesis, a thorough study of thermal conductivity in superlattices has been established, starting first with a deriving the general formula of thermal conductivity across bulks by solving Boltzmann's equation for phonon propagation in crystals. then since the resulting formula is a function of phonon scattering relaxation times the scattering mechanisms were investigated to find the relaxation time of each possible phonon process. afterwards an explanation of the contribution of thermal conductivity from each of the high symmetry directions is presented. the model we adopt was developed by Callaway who reasonably solves Boltzmann equation for phonons with taking into account the physical difference between the normal nature of the normal processes, which tend to displace Plank's distribution function from equilibrium, and the resistive nature of other processes, which tend to restore it back. Nevertheless, Callaway's model presents serious deficiencies that limit its applicability: a) it ignores possible differences between the two transverse velocities, b) it ignores the anisotropic nature of the phonon eigenfrequencies in the Brillouin zone that indicates a directional-dependent c) it uses Debye-like phonon dispersion relations that are reliable at very low temperatures only, and d) it uses inaccurate expressions for intrinsic phonon relaxation times with free adjustable parameters.
We then apply some adjustments to the vibrational parameters to show their dependence on temperature to establish better accuracy. The obtained model definitely presents excellent improvement in the match between the curve obtained by calculations and the expected experimental values. The previous study by Callaway's model for the calculation of the lattice thermal conductivity (κ) has shown to be correct but at low temperatures only. The use of temperature dependent variables fixes the deviations in the thermal conductivity curve at high temperatures. On the

basis of the adiabatic bond charge dynamical matrix, we derived directional and temperature-dependent phonon group velocities and lattice vibration parameters, and relaxation times associated with the intrinsic phonon decay mechanisms, with adopting Callaway's solution to Boltzmann equation. The modified Callaway's model is applied to describe the observed effects of crystallographic orientation and isotope composition on κ of Germanium. Satisfactory agreement is obtained between theory and experiment in the full temperature range demonstrating the importance of the modifications we have made in Callaway's model. With these modifications, the model accounts for the physical natures of the various phonon processes involved in the heat transport and describe the directional dependent κ in the full temperature range in a predictive fashion.

This thesis has also demonstrated a new model for thermal conductivity in superlattices using a mixed mode of transport of phonons across these superlattices. An interplay between a coherent and an incoherent transport is used as well as usage of temperature dependent parameters in the thermal conductivity formula. Relaxation times of different processes including mainly phonon boundary scattering as well as phonon-phonon scatterings are calculated and plugged in the thermal conductivity formula. Assuming that the phonon heat transport through the superlattice interfaces is either purely incoherent or purely coherent. A comparison between the derived theoretical curves and previously reported experimental data showed that both assumptions cannot reproduce the experimental measurements in the full temperature range. The assumption that the phonon heat transport is purely incoherent is appropriate to describe only high temperature cross-plane thermal conductivities of superlattices of period thicknesses not smaller than 30 nm, whereas the assumption that the phonon heat transport is purely coherent is expedient for the prediction of only low temperature cross-plane thermal conductivities of superlattices of very small periods. Then, we have developed a model based on the assumption that the

overall phonon heat transport is a mixture of coherent and incoherent phonon transport modes. We have demonstrated the accuracy and wide scope of the developed model with reference to experimental data regarding the effects of the period thickness and temperature on the cross-plane thermal conductivities of $Si/Si_{0.7}Ge_{0.3}$ and $Si_{0.84}Ge_{0.16}/Si_{0.76}Ge_{0.3}$ superlattices. The reported experimental measurements, for all cases could be well reproduced by the developed model in the full temperature range. We could also demonstrate that the phonon heat transport in a superlattice can be purely incoherent at sufficiently high temperatures, but never purely coherent.

Despite the accomplishments done in this thesis in providing a well-fit theoretical model for thermal conductivity in superlattices, many parts of the study still require detailed investigations. Although the results presented excellent fits at periods of 7.5 and 15nm, a problem arouse at higher thicknesses where fittings started to become poor, which is probably due to some non-accurate theories in the used parameters. For instance, it is necessary to establish a theoretical technique for calculating the elastic and anharmonic interactions of the phonons at the two sides of an interface between two materials in order to get the contribution of phonon -phonon interaction in each material. In addition, how to set up an atomistic transport theory by incorporating non linearity in the quantum regime is still a challenge. The precise calculation of the surface phonon characteristics and their contribution to the thermodynamic function of a crystal having a size of a few tens of nano-meters is also a challenge. The problem of atomistic simulation of the interaction of phonons with other elementary excitations and the consequent effect on the lattice thermal conductivity also deserves further systematic theoretical investigations. The relaxation time approximation also presents different limitations for varying distributions of phonons.

CHAPTER VI

BIBLIOGRAPHY

BIBLIOGRAPHY

[1] Gang Chen. Heat transfer in micro-and nanoscale photonic devices. *Annual Review of Heat Transfer*, 7(7), 1996.

[2] Gang Chen. Thermal conductivity and ballistic-phonon transport in the cross-plane direction of superlattices. *Physical Review B*, 57(23):14958, 1998.

[3] Per Hyldgaard and GD Mahan. Phonon superlattice transport. *Physical Review B*, 56(17):10754, 1997.

[4] David G Cahill, Kenneth Goodson, and Arunava Majumdar. Thermometry and thermal transport in micro/nanoscale solid-state devices and structures. *Journal of Heat Transfer*, 124(2):223–241, 2002.

[5] Terry M Tritt. *Thermal conductivity: theory, properties, and applications*. Springer, 2005.

[6] TC Harman, PJ Taylor, MP Walsh, and BE LaForge. Quantum dot superlattice thermoelectric materials and devices. *science*, 297(5590):2229–2232, 2002.

[7] Gang Chen. *Nanoscale energy transport and conversion: a parallel treatment of electrons, molecules, phonons, and photons*. Oxford University Press, 2005.

[8] P Yashar, SA Barnett, J Rechner, and WD Sproul. Structure and mechanical properties of polycrystalline crn/tin superlattices. *Journal of Vacuum Science & Technology A*, 16(5):2913–2918, 1998.

[9] Vladimir V Mitin, Viatcheslav A Kochelap, and Michael A Stroscio. *Introduction to nanoelectronics: science, nanotechnology, engineering, and applications*. Cambridge University Press, 2008.

[10] Gyaneshwar P Srivastava. *The physics of phonons*. Taylor & Francis, 1990.

[11] Martin Maldovan. Narrow low-frequency spectrum and heat management by thermocrystals. *Physical review letters*, 110(2):025902, 2013.

[12] A Ward and DA Broido. Intrinsic phonon relaxation times from first-principles studies of the thermal conductivities of si and ge. *Physical Review B*, 81(8):085205, 2010.

[13] HBG Casimir. Note on the conduction of heat in crystals. *Physica*, 5(6):495–500, 1938.

[14] MG Holland. Analysis of lattice thermal conductivity. *Physical Review*, 132(6):2461, 1963.

[15] M Asen-Palmer, K Bartkowski, E Gmelin, M Cardona, AP Zhernov, AV Inyushkin, A Taldenkov, VI Ozhogin, KM Itoh, and EE Haller. Thermal conductivity of germanium crystals with different isotopic compositions. *Physical Review B*, 56(15):9431, 1997.

[16] Peter Carruthers. Theory of thermal conductivity of solids at low temperatures. *Reviews of Modern Physics*, 33(1):92, 1961.

[17] JS Dugdale and DKC MacDonald. Lattice thermal conductivity. *Physical Review*, 98(6):1751, 1955.

[18] SM Lee, David G Cahill, and Rama Venkatasubramanian. Thermal conductivity of si-ge superlattices. *Applied physics letters*, 70(22):2957–2959, 1997.

[19] Gang Chen. Phonon transport in low-dimensional structures. *Semiconductors and Semimetals*, 71:203–259, 2001.

[20] Ziheng Yang. Paml 4: phylogenetic analysis by maximum likelihood. *Molecular biology and evolution*, 24(8):1586–1591, 2007.

[21] FX Alvarez, J Alvarez-Quintana, D Jou, and J Rodriguez Viejo. Analytical expression for thermal conductivity of superlattices. *Journal of Applied Physics*, 107(8):084303, 2010.

[22] David G Cahill, Wayne K Ford, Kenneth E Goodson, Gerald D Mahan, Arun Majumdar, Humphrey J Maris, Roberto Merlin, and Simon R Phillpot. Nanoscale thermal transport. *Journal of Applied Physics*, 93(2):793–818, 2003.

[23] Gerald Mahan, Brian Sales, and Jeff Sharp. Thermoelectric materials: New approaches to an old problem. *Physics Today*, 50(3), 1997.

[24] Xiangfan Xu, Luiz FC Pereira, Yu Wang, Jing Wu, Kaiwen Zhang, Xiangming Zhao, Sukang Bae, Cong Tinh Bui, Rongguo Xie, John TL Thong, et al. Length-dependent thermal conductivity in suspended single-layer graphene. *Nature communications*, 5, 2014.

[25] M Kazan, E Moussaed, R Nader, and P Masri. Elastic constants of aluminum nitride. *physica status solidi (c)*, 4(1):204–207, 2007.

[26] DD Betts, AB Bhatia, and Max Wyman. Houston's method and its application to the calculation of characteristic temperatures of cubic crystals. *Physical Review*, 104(1):37, 1956.

[27] Joseph Callaway. Model for lattice thermal conductivity at low temperatures. *Physical Review*, 113(4):1046, 1959.

[28] John M Ziman. *Electrons and phonons: the theory of transport phenomena in solids*. Oxford University Press, 1960.

[29] B Abeles. Lattice thermal conductivity of disordered semiconductor alloys at high temperatures. *Physical Review*, 131(5):1906, 1963.

[30] Z Alameh and M Kazan. Predictive calculation of the lattice thermal conductivity with temperature-dependent vibrational parameters. *Journal of Applied Physics*, 112(12):123506–123506, 2012.

[31] Robert W Keyes. High-temperature thermal conductivity of insulating crystals: relationship to the melting point. *Physical Review*, 115(3):564, 1959.

[32] MN Touzelbaev, P Zhou, R Venkatasubramanian, and KE Goodson. Thermal characterization of bi2te3/sb2te3 superlattices. *Journal of Applied Physics*, 90(2):763–767, 2001.

[33] DT Morelli, JP Heremans, and GA Slack. Estimation of the isotope effect on the lattice thermal conductivity of group iv and group iii-v semiconductors. *Physical Review B*, 66(19):195304, 2002.

[34] Holger T Grahn. *Semiconductor superlattices: growth and electronic properties*. World Scientific, 1995.

[35] Ali Shakouri. Recent developments in semiconductor thermoelectric physics and materials. *Materials Research*, 41(1):399, 2011.

[36] Benoit Latour, Sebastian Volz, and Yann Chalopin. Microscopic description of coherent transport by thermal phonons. *arXiv preprint arXiv:1311.5045*, 2013.

[37]

[38] Eric Pop. Energy dissipation and transport in nanoscale devices. *Nano Research*, 3(3):147–169, 2010.

[39] M Kazan, G Guisbiers, S Pereira, MR Correia, P Masri, A Bruyant, S Volz, and P Royer. Thermal conductivity of silicon bulk and nanowires: Effects of

isotopic composition, phonon confinement, and surface roughness. *Journal of Applied Physics*, 107(8):083503, 2010.

[40] Scott T Huxtable, Alexis R Abramson, Chang-Lin Tien, Arun Majumdara, Chris LaBounty, Xiaofeng Fan, Gehong Zeng, John E Bowers, Ali Shakouri, and Edward T Croke. Thermal conductivity of siõsige and sigeõsige superlattices. *Applied Physics Letters*, 80(10), 2002.

[41] Pramod Reddy, Kenneth Castelino, and Arun Majumdar. Diffuse mismatch model of thermal boundary conductance using exact phonon dispersion. *Applied Physics Letters*, 87(21):211908, 2005.

[42] M Kazan and P Masri. The contribution of surfaces and interfaces to the crystal thermal conductivity. *Surface Science Reports*, 69(1):1–37, 2014.

[43] M Kazan. Interpolation between the acoustic mismatch model and the diffuse mismatch model for the interface thermal conductance: Application to inn/gan superlattice. *Journal of Heat Transfer*, 133(11):112401, 2011.

[44] GH Zhu, H Lee, YC Lan, XW Wang, G Joshi, DZ Wang, J Yang, D Vashaee, H Guilbert, A Pillitteri, et al. Increased phonon scattering by nanograins and point defects in nanostructured silicon with a low concentration of germanium. *Physical review letters*, 102(19):196803, 2009.

[45] Ramez Cheaito, John C Duda, Thomas E Beechem, Khalid Hattar, Jon F Ihlefeld, Douglas L Medlin, Mark A Rodriguez, Michael J Campion, Edward S Piekos, and Patrick E Hopkins. Experimental investigation of size effects on the thermal conductivity of silicon-germanium alloy thin films. *Physical review letters*, 109(19):195901, 2012.

[46] David G Cahill, Fumiya Watanabe, Angus Rockett, and Cronin B Vining. Thermal conductivity of epitaxial layers of dilute sige alloys. *Physical Review B*, 71(23):235202, 2005.

[47] A Iskandar, A Abou-Khalil, M Kazan, W Kassem, and S Volz. On the interplay between phonon-boundary scattering and phonon-point-defect scattering in sige thin films. *Journal of Applied Physics*, 117(12):125102, 2015.